Supporting Information

for

Design and Synthesis of Thiophene-Based C_2-Symmetric Chiral Phosphoric Acids on a Decahydroquinoxaline scaffold for Stereoselective Transformations

Margherita Gazzotti,[a] Vincenzo Mirco Abbinante,[b] Fabrizio Medici,[a] Sara Ghirardi,[b] Sergio Rossi,*[a]
Tiziana Benincori,[b] Roberto Cirilli[c] and Maurizio Benaglia*[a]

[a] Dipartimento di Chimica, Università degli Studi di Milano, via Golgi 19, 20133 Milano, Italy

[b] Dipartimento di Scienza ed Alta Tecnologia, Università degli Studi dell'Insubria, Via Valleggio 11, 22100 Como, Italy

[c] Dipartimento del Farmaco, Istituto Superiore di Sanità, Viale Regina Elena 299, 00161 Roma, Italy

Table of Contents

1. General method

Dry solvents: Dry solvents were purchased and stored under nitrogen over molecular sieves (bottles with crown caps).

Chromatographic purification: Purification of products was performed by column chromatography with flash technique (according to the Still method) using as stationary phase silica gel 230-400 mesh purchase from MERCK.

Thin-Layer Chromatography (TLC): Reactions and chromatographic purifications were monitored by analytical thin-layer chromatography (TLC) using silica gel 60 F254 pre-coated glass plates (0.25 mm thickness) and visualized using UV light (365 nm).

NMR spectra: ^{1}H-NMR spectra were recorded on spectrometers operating at 300 MHz (Brucker Avance 300). The chemical shifts are reported in ppm (δ), with the solvent reference relative to tetramethyl silane (TMS) employed as the internal standard ($CDCl_3$ δ = 7.26 ppm). ^{13}C-NMR spectra were recorded on a 300 MHz (Brucker Avance 300) operating at 75 MHz, with complete proton decoupling. Carbon chemical shifts are reported in ppm (δ) relative to TMS with the respective solvent resonance as the internal standard ($CDCl_3$ δ = 77.16 ppm). ^{31}P-NMR spectra were recorded on a 300 MHz (Bruker Avance 300) spectrometer operating at 121.2 MHz, with complete proton decoupling. Phosphorous chemical shifts are reported in ppm (δ) relative to H_3PO_4 as internal standard. ^{1}H-NMR, ^{13}C-NMR and ^{31}P-NMR of all the synthetized compounds were recorded in $CDCl_3$.

Mass spectra: High resolution mass spectra (HRMS) were acquired using a Q-TOF Synapt G2-Si/HDMS 8K instrument available at the MS facility of the Unitech COSPECT at the University of Milan.

Optical rotations: Optical rotations were obtained on a JASCO P-1030 polarimeter (Series: A014060839) at 589 nm using a 1 mL cell, with a length of 1 dm.

Melting points: Melting points were measured using Stuart SMP3 melting point apparatus, provided by STUART SCIENTIFIC.

High Performance Liquid Chromatography (HPLC): HPLC traces of both pure enantiomeric forms of compound **9** were acquired using a stainless-steel Chiralpak IB column (250 × 4.6 mm, 5 µm) supplied by Chiral Technologies Europe (Illkirch-Graffenstaden, France). Analytical HPLC experiments were performed using a PerkinElmer 200 LC pump equipped with a Rheodyne injector fitted with a 50 µL sample loop, a Dionex CC-100 column oven, and a Jasco CD-2095 Plus UV/CD detector. Chromatographic data were acquired and processed using Clarity software (DataApex). HPLC analyses of compounds **15aa-ad** were performed using Agilent 1100 equipped with a quaternary pump and autosampler or 1200 series HPLC equipped with a binary pump. Chiral chromatographic separations followed by UV detection were performed using HPLC columns with chiral stationary phase with dimensions 250 x 4.6mm ID (Daicel CHIRALCEL OD-H or Lux Cellulose-1 3 µm). The specific operating conditions for each product are reported from time to time.

Circular dichroism spectra: Circular dichroism spectra were measured in a 0.1 cm path length quartz cell at 25 ◦C using a Jasco (Tokyo, Japan) model J-700 spectropolarimeter. The intensities of spectra are expressed as ellipticity values (mdeg).

2. Experimental Procedures and Characterization Data

2.1. Synthesis of Chiral Phosphoric Acid 2

Synthesis of compound 4

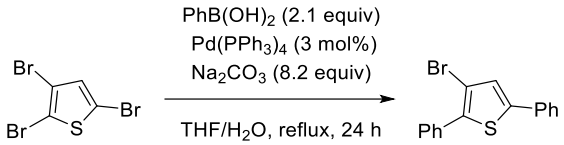

3 **4**

2,3,5-tribromothiophene **3** (1 g, 3.11 mmol, 1 equiv) was added under nitrogen atmosphere to a biphasic mixture of anhydrous THF (0.23 M) and 20% w/v sodium carbonate aqueous solution (13.5 mL, 8.2 equiv), previously degassed with nitrogen for 20 minutes. Phenylboronic acid (758.4 mg, 6.22 mmol, 2.1 equiv) and $Pd(PPh_3)_4$ (250.3 mg, 0.093 mmol, 0.03 equiv) were subsequently added, and the mixture was refluxed for 24 hours. Then THF was removed under reduced pressure, and the residue was extracted with CH_2Cl_2 (3 x 15 mL). The organic layers were collected, washed with brine (15 ml), dried over $MgSO_4$, filtered, and concentrated under vacuo. The residue was purified by column chromatography (eluent: hexane), obtaining the 3-bromo-2,5-diphenylthiophene **4** as a light-yellow liquid (59% yield).

^{1}H-NMR (300 MHz, $CDCl_3$) δ 7.75 – 7.66 (m, 2H), 7.65 – 7.52 (m, 2H), 7.50 – 7.27 (m, 7H).

The data are in agreement with those reported in the literature.[1]

Synthesis of compound 5

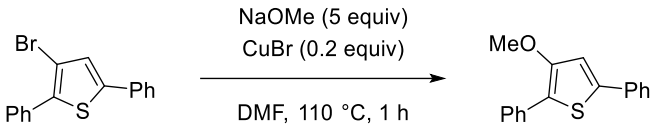

4 **5**

Sodium methoxide was prepared by dissolving sodium (181.6 mg, 7.93 mmol, 5 equiv) in dry methanol (6 mL) under nitrogen atmosphere at room temperature. When all the sodium was consumed, the sodium methoxide solution was added to of dry DMF. Then 2,5-diphenyl-3-bromothiophene **4** (500 mg, 1.58 mmol, 1 equiv) and copper(I) bromide (45.3 mg, 0.316 mmol, 0.2 equiv) were added, and the reaction mixture was stirred at 110 °C for 30 minutes. The mixture was then filtered on a small pad of celite and washed with *n*-hexane (12 mL). The liquor was then washed with water (12 mL), and the aqueous phase was extracted twice with *n*-hexane (2 x 15 mL). The collected organic layers were dried over $MgSO_4$ and concentrated under reduced pressure. The residue was purified by column chromatography on silica gel (eluent: hexane/CH_2Cl_2 8:2). 3-methoxy-2,5-diphenylthiophene **5** was obtained as a yellow solid (62% yield).

^{1}H-NMR (300 MHz, $CDCl_3$) δ 7.77 (d, *J* = 8.2 Hz, 2H), 7.62 (d, *J* = 7.8 Hz, 2H), 7.50 – 7.10 (m, 7H), 3.97 (s, 3H).

The data are in agreement with those reported in the literature.[2]

Synthesis of compound 6

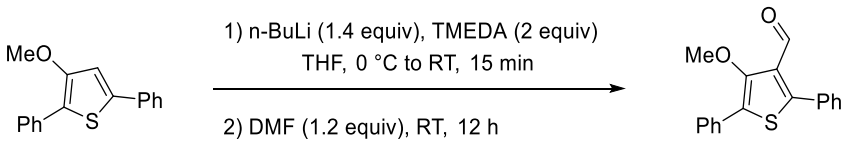

5 **6**

In a flame-dried Schlenk tube, under nitrogen atmosphere, at room temperature 3-methoxy-2,5-diphenylthiophene **5** (250 mg, 0.94 mmol, 1 equiv) was dissolved in anhydrous THF (0.064 M) followed by the addition of distilled TMEDA (280.2 µL, 1.87 mmol, 2 equiv). The solution was cooled down to 0 °C, and then *n*-BuLi solution (1.6 M in THF, 800 µL, 1.305 mmol, 1.4 equiv) was added dropwise. The mixture was left stirring for 15 minutes at 0 °C and then it was warmed up to room temperature. Dry DMF (86.9 µL, 1.12 mmol, 1.2 equiv) was then added dropwise, and the reaction mixture was left stirring for 12 hours at room temperature. A saturated solution of NH_4Cl (15 mL) was then added to quench the reaction and THF was removed under vacuum. After the aqueous solution was extracted with CH_2Cl_2 (3 x 15 mL) and the collected organic phases were dried over $MgSO_4$, filtered and concentrated under reduced pressure. The residue was purified by flash column chromatography (eluent: hexane/CH_2Cl_2 6:4) to give 4-methoxy-2,5-diphenylthiophene-3-carbaldehyde **6** as a yellow solid (57% yield).

Rf = 0.42 (eluent: hexane/DCM 6:4).

^{1}H-NMR (300 MHz, $CDCl_3$) δ 9.91 (s, 1H), 7.81 – 7.71 (m, 2H), 7.60 – 7.41 (m, 7H), 7.37 – 7.30 (m, 1H), 3.85 (s, 3H).

^{13}C-NMR (75 MHz, $CDCl_3$) δ 185.51, 152.83, 152.59, 131.96, 131.61, 130.08, 129.87, 129.60, 129.03, 128.89, 128.82, 127.93, 127.68, 127.56, 61.88.

HRMS (ES/QTOF): calcd m/z for $C_{18}H_{14}O_2S$ $[M+Na]^+$, 317.0615; found, 317.0608

m.p. = 134.3 – 136.2 °C

Synthesis of compound 7

6 **7**

Under nitrogen atmosphere, 650 mg (2.21 mmol, 1 equiv) of 4-methoxy-2,5-diphenylthiophene-3-carbaldehyde **6** were dissolved with 10 mL of dry DCM (to give 0.2 M solution). The reaction mixture was cooled down to -78 °C, then 2.65 mL (2.65 mmol, 2 equiv) of 1M solution of BBr_3 in DCM were added dropwise. The resulting mixture was then stirred at room temperature for 19 hours. The reaction was quenched with a saturated aqueous solution of $NaHCO_3$; the two phases were separated, and the aqueous phase was then extracted three times with DCM (3 x 15 mL). Organic phases were collected, dried over sodium sulfate, filtered and concentrated under reduced pressure. The crude was purified by column chromatography on silica gel (eluent: hexane/DCM 6:4). Product **7** was obtained as an orange solid in quantitative yield.

Rf = 0.38 (eluent: hexane/DCM 6:4).

^{1}H NMR (300 MHz, $CDCl_3$) δ 9.93 (br s, 1H), 9.88 (s, 1H), 7.86 – 7.76 (m, 2H), 7.63 – 7.47 (m, 5H), 7.41 (t, *J* = 7.7 Hz, 2H), 7.33 – 7.21 (t, *J* = 7.7 Hz, 1H).

^{13}C NMR (75 MHz, $CDCl_3$) δ 189.70, 153.17, 151.71, 132.03, 131.23, 129.89, 129.53, 129.19, 128.75, 126.88, 126.47, 125.05, 116.52.

HRMS (ES/QTOF): calcd m/z for $C_{17}H_{12}O_2S$ $[M+Na]^+$, 303.0458; found, 303.0452

m.p. = 126.8 – 138.2 °C

Synthesis of compound 9

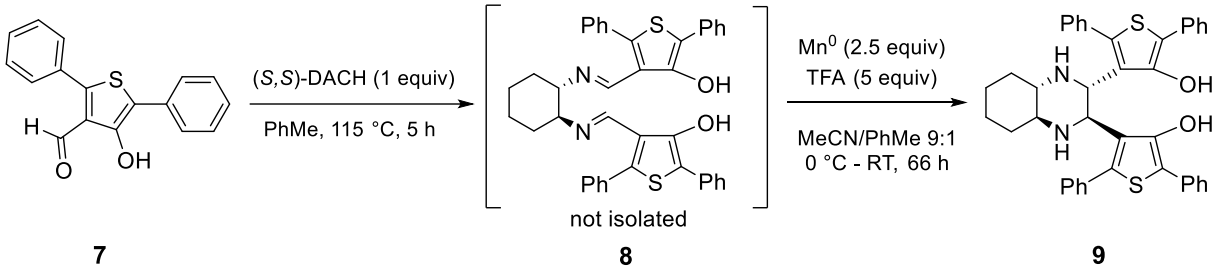

7 **8** **9**

In a round bottom one-neck flask, containing **7** (690 mg, 2.46 mmol, 2.05 equiv), a solution of (*S,S*)-*trans*-1,2-diaminocyclohexane (141.0 mg, 1.23 mmol, 1 equiv) in toluene (6 mL, to give a 0.2 M solution) was added. With a Dean-Stark apparatus, the mixture was refluxed at 115 °C for 5 hours. The mixture was then cooled down to room temperature, and the solvent was removed by evaporation under reduced pressure. The formation of the bis-imine intermediate **8** was verified through ^{1}H-NMR analysis of the resulting crude.

Subsequently, the residue was then dissolved in a 9:1 mixture of dry acetonitrile and dry toluene (20.5 mL, to give 0.06 M solution), which was slowly added under nitrogen atmosphere into a two-neck flask containing manganese powder (170.3 mg, 3.1 mmol, 2.5 equiv). The resulting mixture was cooled down to 0 °C and trifluoroacetic acid (0.5 mL, 6.15 mmol, 5 equiv) was added dropwise over 5 minutes. The resulting mixture was then stirred at room temperature for 24 hours. The reaction was quenched with 150 mL of saturated solution of $NaHCO_3$, the two phases were separated, and the aqueous phase was then extracted three times with ethyl acetate (3 x 50 mL). The collected organic phases were dried over sodium sulfate, filtered and concentrated under vacuum. The crude was purified by flash column chromatography on silica gel (eluent: from hexane/DCM 8:2 to DCM). Desired product **9** was obtained as a pale-yellow solid with 87% yield.

Rf = 0.3 (eluent: hexane/DCM 1:1)

^{1}H NMR (300 MHz, $CDCl_3$) δ 10.41 (br s, 2H), 7.66 (s, 4H), 7.41 (s, 4H), 7.29 – 6.91 (m, 12H), 4.68 (s, 2H), 4.19 (s, 2H), 2.61 (s, 2H), 2.11 (s, 2H), 1.80 – 1.74 (m, 4H), 1.36 (d, *J* = 17.5 Hz, 4H).

^{13}C NMR (75 MHz, $CDCl_3$) δ 150.60, 137.76, 133.41, 132.99, 128.53, 128.20, 127.86, 126.37, 125.69, 125.05, 116.39, 59.57, 56.70, 31.40, 24.30.

HRMS (ES/QTOF): calcd m/z for $C_{40}H_{36}N_2O_2S_2$ $[M+H]^+$, 641.2298; found, 641.2299

$[\alpha]_D^{20}$ = + 246.64 (c = 1.0, $CHCl_3$)

m.p. = 244.8 – 246.9 °C

Synthesis of compound 11

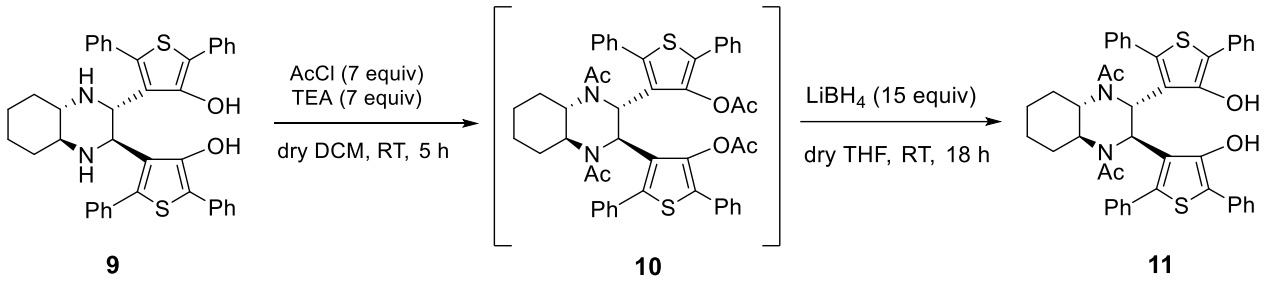

To a 0.1 M solution of compound **9** (550.0 mg, 0.86 mmol, 1.0 equiv) in dry dichloromethane (8.6 mL), triethylamine (0.8 mL, 6.01 mmol, 7.0 equiv) was added. Then, acetyl chloride (0.4 mL, 6.01 mmol, 7.0 equiv) was added dropwise to the mixture and, after 5 hours at room temperature, 10 mL of saturated solution of $NaHCO_3$ were added. The two phases were separated, and the aqueous phase was then extracted three times with dichloromethane (3 x 20 mL) and the combined organic layers were dried over sodium sulphate, filtered and concentrated under vacuum. The crude compound **10** was used directly in the subsequent reaction without further purification.

$LiBH_4$ (216.0 mg, 9.93 mmol, 15.0 equiv) was slowly added to a solution of **10** (535.0 mg, 0.66 mmol, 1.0 equiv) in dry THF (7 mL). The mixture was left under stirring for 16 hours. 20 mL of DCM and 20 mL of an aqueous solution of HCl 1 M were then added. The two phases were separated, and the aqueous phase was then extracted three times with DCM (3 x 20 mL) The collected organic phases were then dried over magnesium sulfate, filtered and concentrated under reduced pressure. The crude was purified by flash column chromatography on silica gel (eluent: from hexane/ethyl acetate 9:1 to hexane/ethyl acetate 6:4). Product **11** was obtained as white solid with 76% yield.

Rf = 0.35 (eluent: hexane/ ethyl acetate 8:2)

^{1}H NMR (300 MHz, $CDCl_3$) δ 7.77 – 7.65 (m,4H), 7.55 (s, 1H), 7.44 – 7.30 (m, 10H), 7.28 – 7.21 (m, 2H), 7.18 – 7.12 (m, 3H), 5.69 (s, 2H), 2.56 (d, *J* = 10.2 Hz, 2H), 1.66 (s, 2H), 1.60 (s, 6H), 1.32 – 1.13 (m, 4H).

^{13}C NMR (75 MHz, $CDCl_3$) δ 174.42, 147.87, 135.91, 133.96, 132.95, 130.20, 129.60, 129.06, 128.84, 128.75, 128.57, 127.41, 127.06, 126.73, 118.92, 59.70, 56.82, 32.67, 25.22, 22.15.

HRMS (ES/QTOF): calcd m/z for $C_{44}H_{40}N_2O_4S_2$ $[M-H]^-$, 723.2350; found, 723.2343

$[\alpha]_D^{20}$ = + 23.01 (c = 1.0, $CHCl_3$)

m.p.= 136.3 – 138.1 °C

Synthesis of compound 2

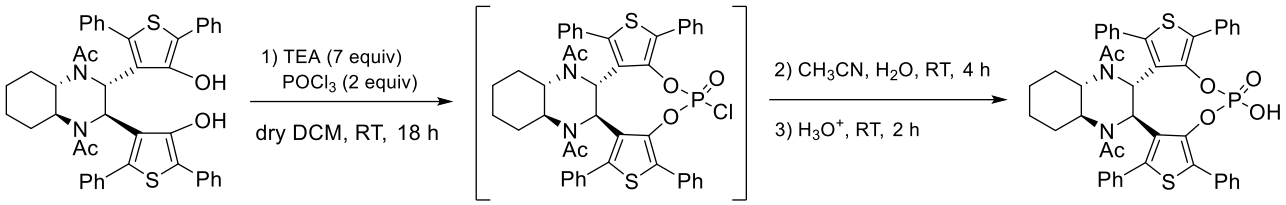

11 **12** **2**

A solution of $POCl_3$ (0.41 mL of a 1 M solution in DCM, 0.410 mmol, 2.0 equiv) in dry DCM (2 mL) was added dropwise at 0 °C to a solution of diol **11** (149.0 mg, 0.205 mmol, 1.0 equiv) and dry triethylamine (0.2 mL, 1.44 mmol, 7.0 equiv) in dry DCM (2 mL). Then, the reaction mixture was stirred for 18 hours at room temperature.

2 mL of acetonitrile and 1 mL of water were then added, and the reaction mixture was stirred for additional 4 hours at room temperature. Then 10 mL of DCM were added, and the reaction mixture was washed with 20 mL of an aqueous solution of HCl 1 M. The two phases were separated, and the aqueous phase was extracted three times with DCM (3 x 20 mL). The organic phases were collected, dried over magnesium sulfate, filtered and concentrated under reduced pressure. The crude was purified by flash column chromatography on silica gel (eluent: from DCM to DCM/methanol 95:5). The product **2** (140.0 mg, 0.193 mmol) was obtained as white solid with 86% yield.

Rf = 0.30 (eluent: ethyl acetate/methanol 95:5)

^{1}H NMR (300 MHz, $CDCl_3$) δ 7.75 – 7.51 (m, 10H), 7.16 – 7.01 (m, 5H), 6-96 – 6.85 (m, 2H), 6.79 – 6.69 (m, 3H), 6.52 (d, *J* = 12.6 Hz, 1H), 6.32 (s, 1H), 5.13 (d, *J* = 12.8 Hz, 1H), 3.76 (d, *J* = 11.7 Hz, 1H), 3.03 (s, 1H), 2.62 (d, *J* = 11.6 Hz, 1H), 2.08 (s, 3H), 1.83 (s, 3H), 1.72 (d, *J* = 11.9 Hz, 1H), 1.61 (d, *J* = 12.0 Hz, 1H), 1.14 (s, 1H), 0.98 (s, 1H).

^{13}C NMR (75 MHz, $CDCl_3$) δ 176.09, 173.51, 141.89, 141.79, 141.23, 140.59, 140.48, 140.01, 137.82, 137.09, 136.86, 134.70, 134.42, 133.87, 133.27, 133.06, 132.60, 132.39, 132.06, 131.41, 131.04, 130.03, 129.61, 129.07, 128.77, 128.72, 128.43, 128.30, 127.86, 127.75, 127.59, 127.48, 127.43, 125.20, 66.93, 64.62, 59.97, 53.49, 33.08, 31.92, 29.65, 26.42, 24.22, 23.70.

HRMS (ES/QTOF): calcd m/z for $C_{44}H_{39}N_2O_6PS_2$ $[M-H]^-$, 785.1907; found, 785.1901

^{31}P NMR (122 MHz, $CDCl_3$) δ -14.08

$[\alpha]_D^{20}$ = + 152.34 (c = 1.0, $CHCl_3$)

m.p.= 153.8 – 155.2 °C

2.2. Synthesis of *N*-tosyl-imines 13a-c

General procedure [3]

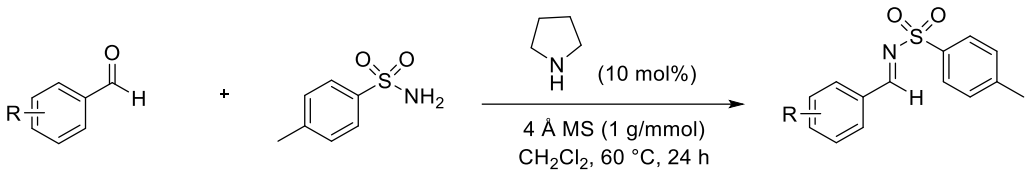

16a-c **13a-c**

In a sealed vial, under nitrogen, to a 0.32 M solution of *p*-toluensulfonamide (2 g, 11.7 mmol, 1 equiv) in dichloromethane with 4 Å molecular sieves (1 g/mmol) aldehyde **16a-c** (14.0 mmol, 1.2 equiv) and pyrrolidine (0.1 mL, 1.17 mmol, 0.1 equiv) were added. The resulting mixture was stirred at 60 °C for 24 hours. The reaction mixture was then filtered through a short pad of Celite and concentrated under reduced pressure. The residue was then dissolved in ethyl acetate and recrystallized for 20 hours adding hexane (ratio ethyl acetate/hexane 3:1). Solvents were then removed with a Pasteur pipette and the residue dried under reduced pressure. To remove residual aldehyde, the residue was left under high vacuum for 24 hours (temperature specified below for each compound). Desired imines **13a-c** were obtained without any further purification.

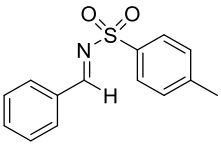

13a

Residual aldehyde **16a** was removed under vacuum at 25 °C.

The desired product **13a** was obtained as a white solid (2.9734 g, 11.5 mmol, 98% yield).

^{1}H-NMR (300 MHz, $CDCl_3$) δ 9.03 (s, 1H), 7.95 – 7.86 (m, 4H), 7.65 – 7.58 (m, 1H), 7.49 (t, *J* = 7.8, 7.8 Hz, 2H), 7.34 (d, *J* = 8.1 Hz, 2H), 2.44 (s, 3H).

The data are in agreement with those reported in the literature.[4]

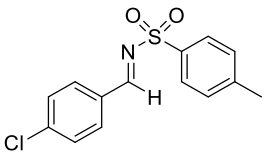

13b

Residual aldehyde **16b** was removed under vacuum at 80 °C.

The desired product **13b** was obtained as a white solid (3.1621 g, 10.8 mmol, 92% yield).

^{1}H-NMR (300 MHz, $CDCl_3$) δ 8.99 (s, 1H), 7.88 (d, *J* = 8.3 Hz, 2H), 7.86 (d, *J* = 8.5 Hz, 2H), 7.46 (d, *J* = 8.5 Hz, 2H), 7.35 (d, *J* = 8.1 Hz, 2H), 2.43 (s, 3H).

The data are in agreement with those reported in the literature.[4]

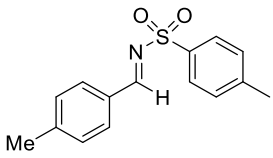

13c

Residual aldehyde **16c** was removed under vacuum at 25 °C. The desired product **13c** was obtained as a white solid (3.0383 g, 11.1 mmol, 95% yield).

^{1}H-NMR (300 MHz, $CDCl_3$) δ 8.99 (s, 1H), 7.88 (d, *J* = 8.0 Hz, 2H), 7.81 (d, *J* = 7.9 Hz, 2H), 7.31 (dd, *J* = 15.4, 8.0 Hz, 4H), 2.43 (d, *J* = 1.7 Hz, 6H).

The data are in agreement with those reported in the literature.[4]

2.3. Stereoselective Friedel-Crafts addition of indoles to *N*-tosyl-imines

General procedure

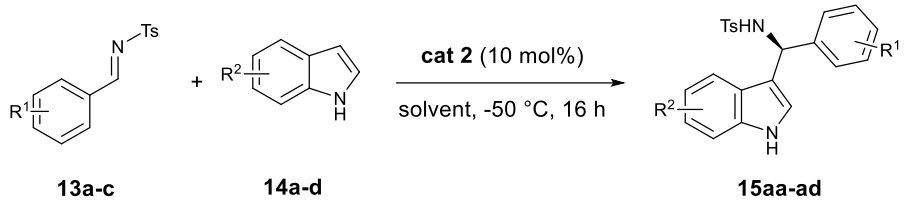

13a-c **14a-d** **15aa-ad**

In a dry Schlenk tube under argon, indole **14a-d** (0.5 mmol, 5 equiv) and chiral phosphoric acid **2** (0.01 mmol, 0.1 equiv) were dissolved in the desired solvent (0.5 mL) and cooled down to -50 °C. A solution (0.5 mL) of the desired imine **13a-c** (0.1 mmol, 1 equiv) was then added and the mixture was stirred for 16 hours. Saturated solution of $NaHCO_3$ (1 mL) was added to quench the reaction, and the mixture was extracted three times with ethyl acetate (3 x 5 mL). The collected organic layers were dried over anhydrous sodium sulphate and then dried under vacuum. The residue was purified by flash column chromatography on silica gel (eluent: hexane/ethyl acetate 3:1) to afford the desired product **15aa-ad**. The yield was calculated on the pure product obtained after column chromatography and the *ee* was evaluated by CSP-HPLC analysis.

Table S1.

Entry	R^1	R^2	Solvent	Product	Yield (%)	*ee* (%)
1	H	H	Toluene	**15aa**	90	72
2	H	H	CH_2Cl_2	**15aa**	98	92
3	4-Cl	H	CH_2Cl_2	**15ba**	82	70
4	4-CH_3	H	CH_2Cl_2	**15ca**	84	86
5	H	5-Br	CH_2Cl_2	**15ab**	88	70
6	H	5-Me	CH_2Cl_2	**15ac**	96	98
7	H	5-OMe	CH_2Cl_2	**15ad**	92	93

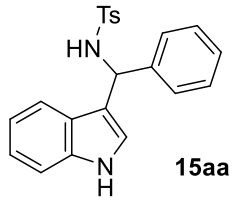

15aa

R_f = 0.18 (eluent: hexane/ethyl acetate 2:1); colorless solid with 98% yield and 92% *ee*. [Daicel Chiralcel OD-H, Hexane/IPA 70:30, 0.6 mL/min, λ = 254 nm, t (minor) = 12.08 min (*R* enantiomer), t (major) = 21.79 min (*S* enantiomer)]

^{1}H-NMR (300 MHz, MeOD) δ 7.54 – 7.44 (m, 2H), 7.28 – 7.19 (m, 4H), 7.19 – 7.10 (m, 3H), 7.10 – 6.98 (m, 3H), 6.91 – 6.80 (m, 1H), 6.61 (d, *J* = 0.9 Hz, 1H), 5.79 (s, 1H), 2.30 (s, 3H).

The data are in agreement with those reported in the literature.[5]

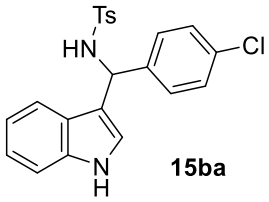

15ba

R_f = 0.30 (eluent: hexane/ethyl acetate 2:1); colorless solid with 82% yield and 70% *ee*. [Phenomenex Lux Cellulose-1 3 µm, Hexane/IPA 6:4, 0.75 mL/min, λ = 254 nm, t (minor) = 10.67 min, t (major) = 15.83 min]

^{1}H-NMR (300 MHz, MeOD) δ 7.50 (d, *J* = 8.1 Hz, 2H), 7.30 – 7.23 (m, 2H), 7.19 (d, *J* = 11.2 Hz, 3H), 7.16 – 7.02 (m, 4H), 6.90 (t, *J* = 7.6 Hz, 1H), 6.64 (s, 1H), 5.80 (s, 1H), 2.35 (s, 3H).

The data are in agreement with those reported in the literature.[5]

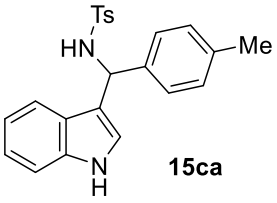

15ca

R_f = 0.26 (eluent: hexane/ethyl acetate 2:1); colorless solid with 84% yield and 86% *ee*. [Phenomenex Lux Cellulose-1 3 µm, Hexane/IPA 70:30, 0.75 mL/min, λ = 254 nm, t (minor) = 11.33 min, t (major) = 19.09 min]

^{1}H-NMR (300 MHz, MeOD) δ 7.53 (d, *J* = 8.3 Hz, 2H), 7.31 (dd, *J* = 8.1, 3.6 Hz, 2H), 7.13 – 6.97 (m, 7H), 6.92 (t, *J* = 7.6 Hz, 1H), 6.71 (s, 1H), 5.81 (s, 1H), 2.37 (s, 3H), 2.32 (s, 3H).

The data are in agreement with those reported in the literature.[5]

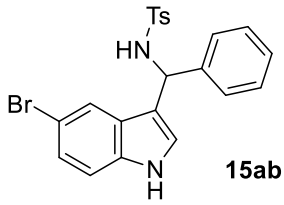

15ab

Rf = 0.32 (eluent: hexane/ethyl acetate 2:1); colorless solid with 88% yield and 70% *ee*. [Daicel Chiralcel OD-H, hexane/IPA 80:20, 1.0 mL/min, λ = 254 nm, t (minor) = 9.10 min, t (major) = 28.25 min]

^{1}H-NMR (600 MHz, $CDCl_3$) δ 8.11 (s, 1H), 7.64 – 7.59 (m, 2H), 7.24 (dd, *J* = 8.6, 1.9 Hz, 1H), 7.22 (s, 5H), 7.21 (s, 1H), 7.17 (d, *J* = 8.6 Hz, 1H), 6.67 (d, *J* = 2.5 Hz, 1H), 5.70 (d, *J* = 6.2 Hz, 1H), 4.98 (d, *J* = 6.2 Hz, 1H), 2.43 (s, 3H).

The data are in agreement with those reported in the literature.[5]

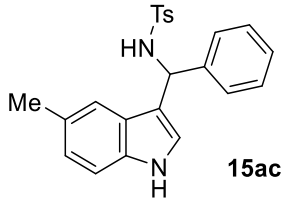

15ac

Rf = 0.28 (eluent: hexane/ethyl acetate 3:1); colorless solid with 96% yield and 98% *ee*. [Daicel Chiralcel OD-H, hexane/IPA 70:30, 0.8 mL/min, λ = 254 nm, t (minor) = 8.27 min, t (major) = 20.61 min]

^{1}H-NMR (300 MHz, $CDCl_3$) δ 7.92 (br, 1H), 7.53 (d, *J* = 7.8 Hz, 2H), 2.27 (s, 3H), 7.16 – 7.20 (m, 5H), 7.06 – 7.10 (m, 3H), 6.92 (d, *J* = 8.7 Hz, 1H), 6.84 (s, 1H), 6.44 (s, 1H), 5.74 (d, *J* = 6.6 Hz, 1H), 5.22 (d, *J* = 6.6 Hz, 1H), 2.34 (s, 3H).

The data are in agreement with those reported in the literature.[5]

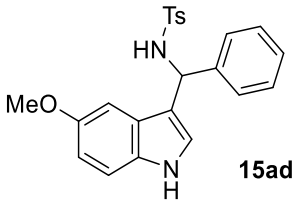

15ad

Rf = 0.42 (eluent: hexane/ethyl acetate 2:1); colorless solid with 92% yield and 94% *ee*. [Daicel Chiralcel OD-H, hexane/IPA 60:40, 0.6 mL/min, λ = 280 nm, t (minor) = 8.44 min, t (major) = 26.76 min]

^{1}H-NMR (300 MHz, $CDCl_3$) δ 8.20 (br, 1H), 7.44 (d, *J* = 7.8 Hz, 2H), 7.03-7.14 (m, 6H), 6.94 (d, *J* = 8.1 Hz, 2H), 6.69-6.73 (m, 2H), 6.44 (d, *J* = 1.8 Hz, 1H), 5.73 (d, *J* = 7.5 Hz, 1H), 5.56 (d, *J* = 7.5 Hz, 1H), 3.63 (s, 3H), 2.23 (s, 3H).

The data are in agreement with those reported in the literature.[5]

3. NMR spectra and HRMS

^{1}H-NMR compound 4

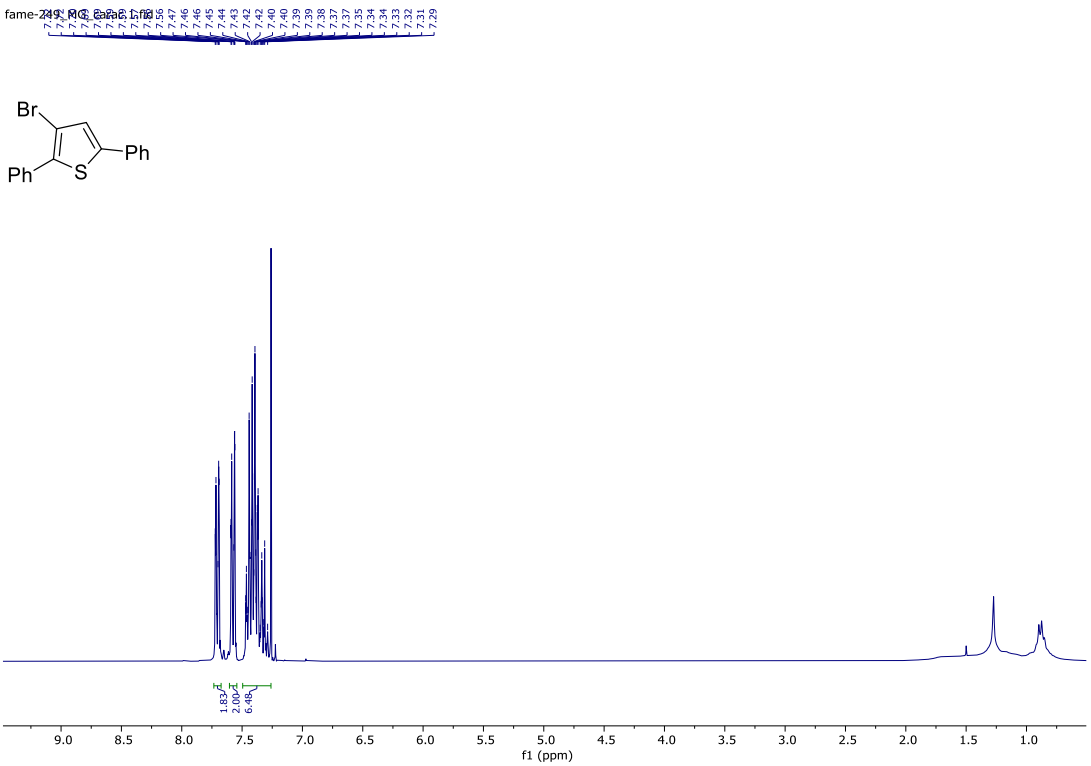

^{1}H-NMR compound 5

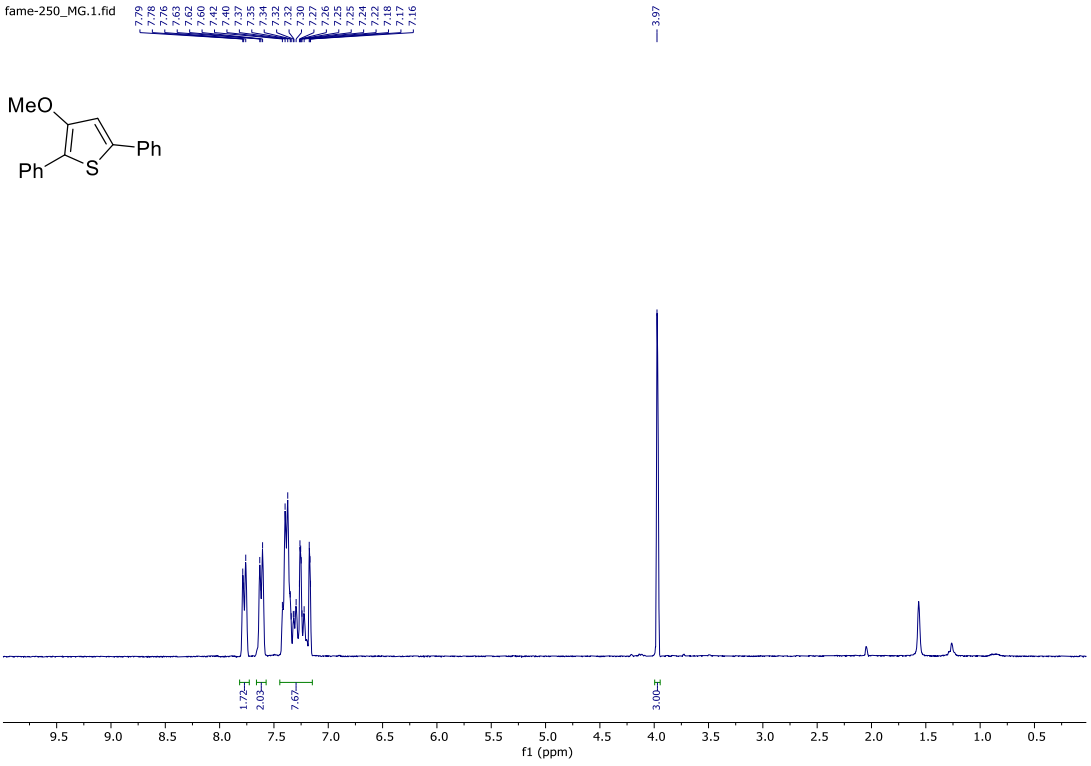

^{1}H-NMR compound 6

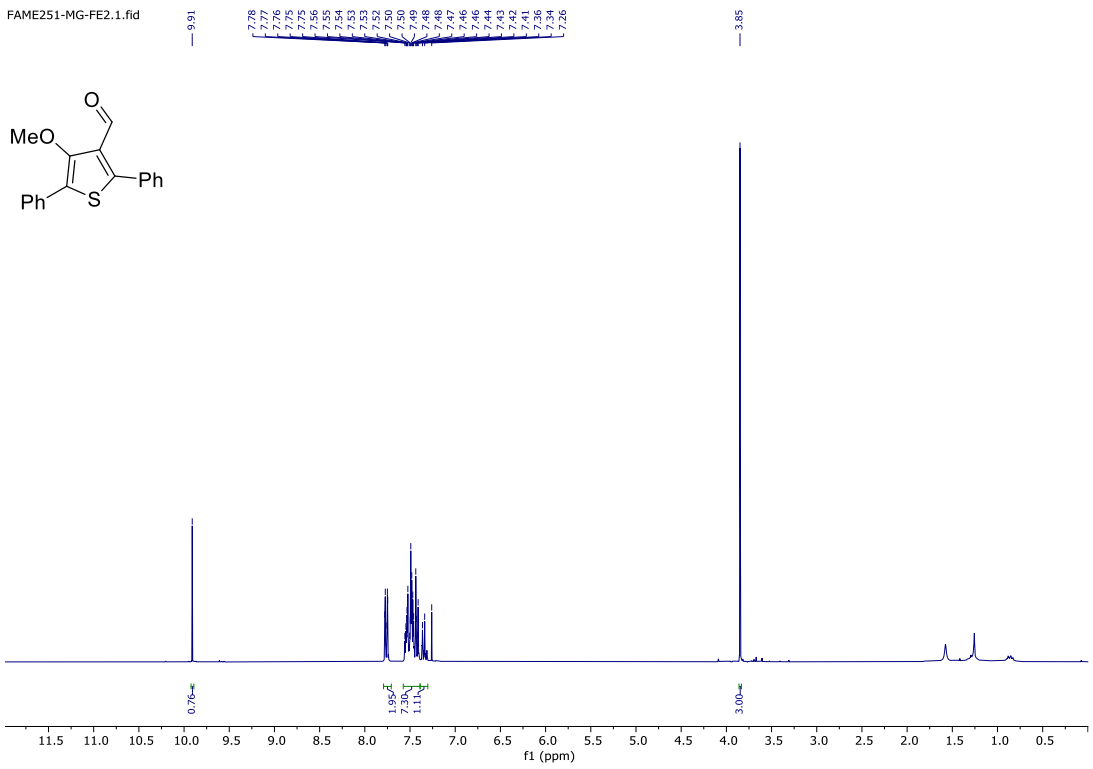

^{13}C-NMR compound 6

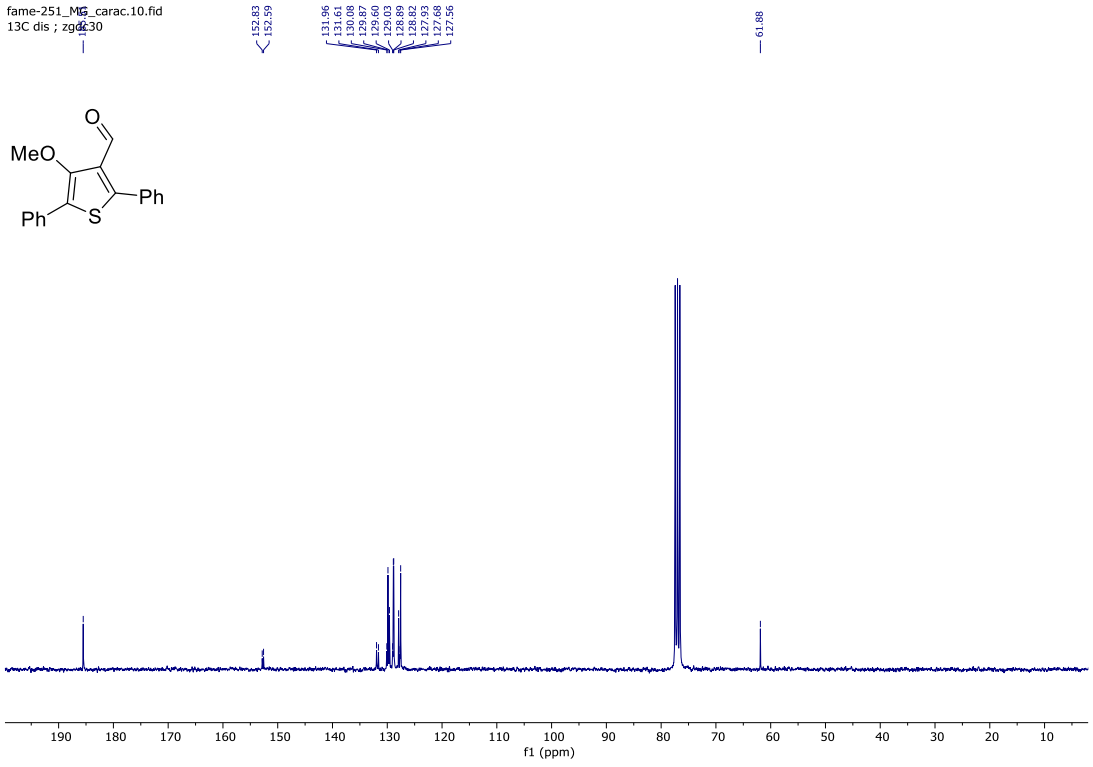

^{1}H-NMR compound 7

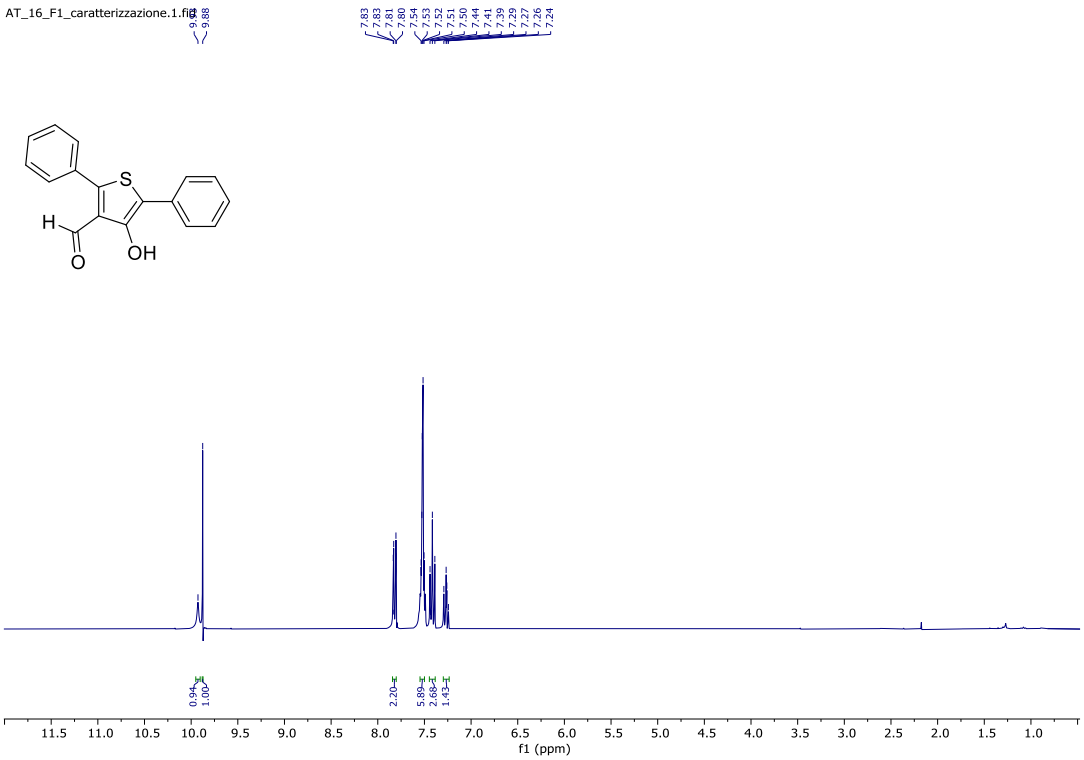

^{13}C-NMR compound 7

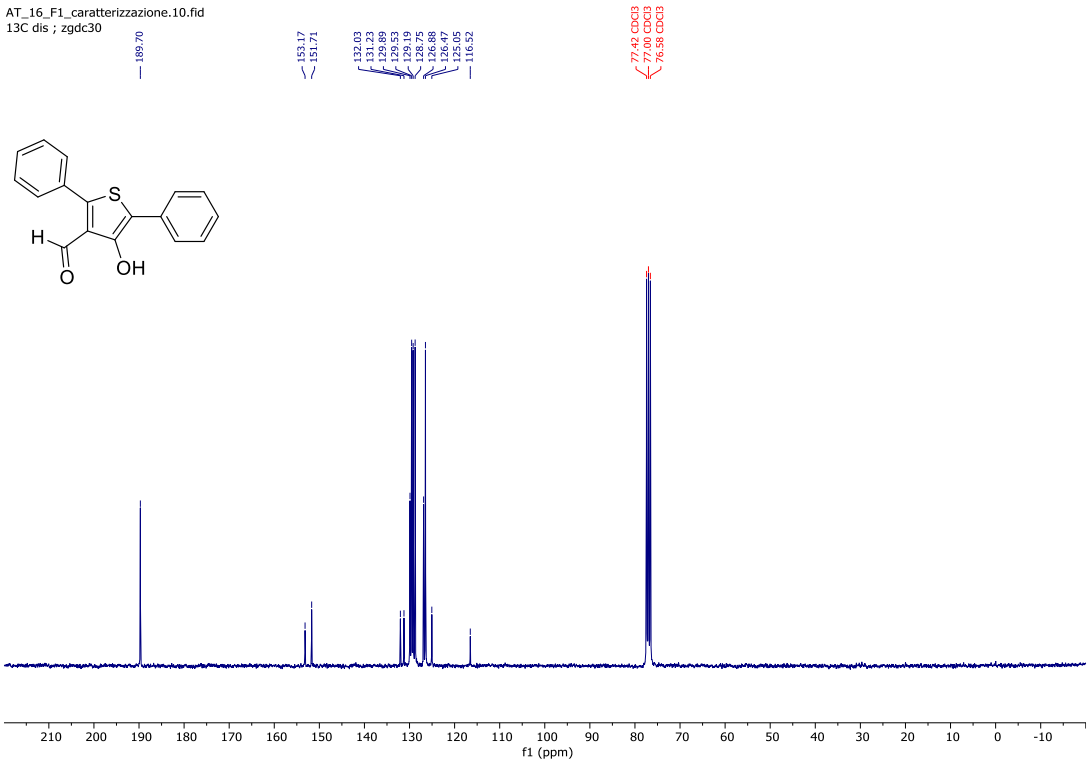

^{1}H-NMR compound 9

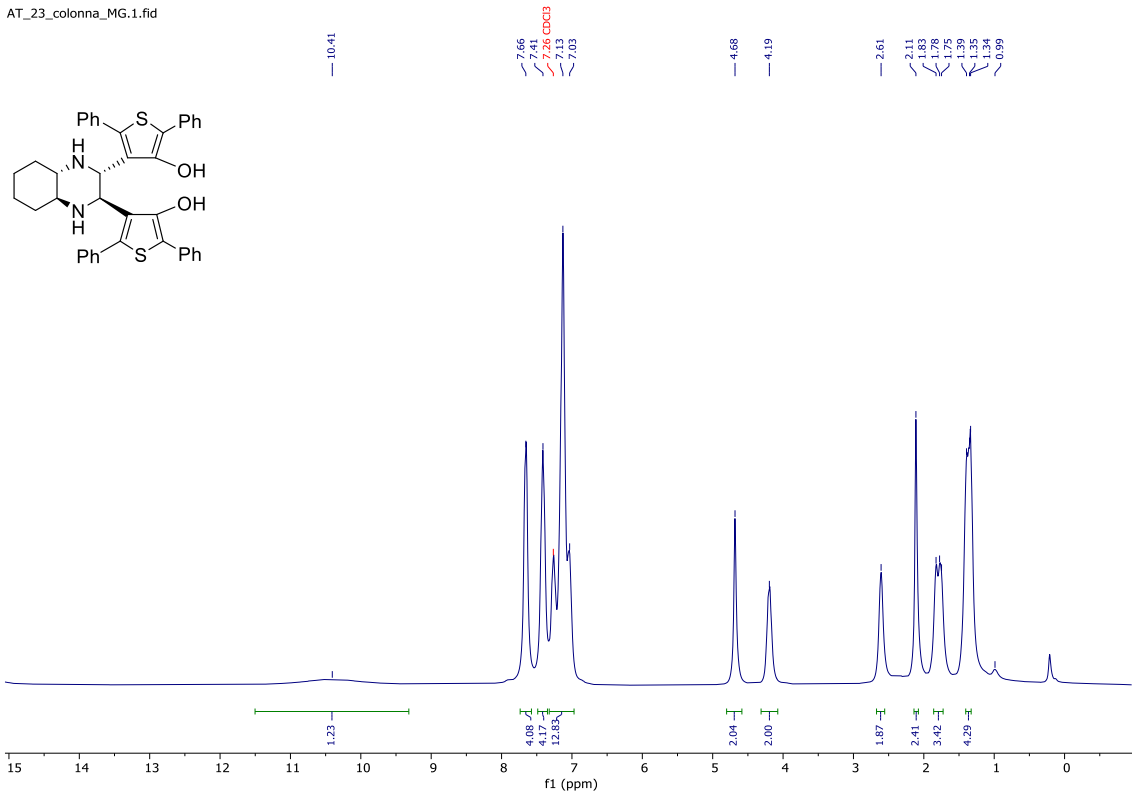

^{13}C-NMR compound 9

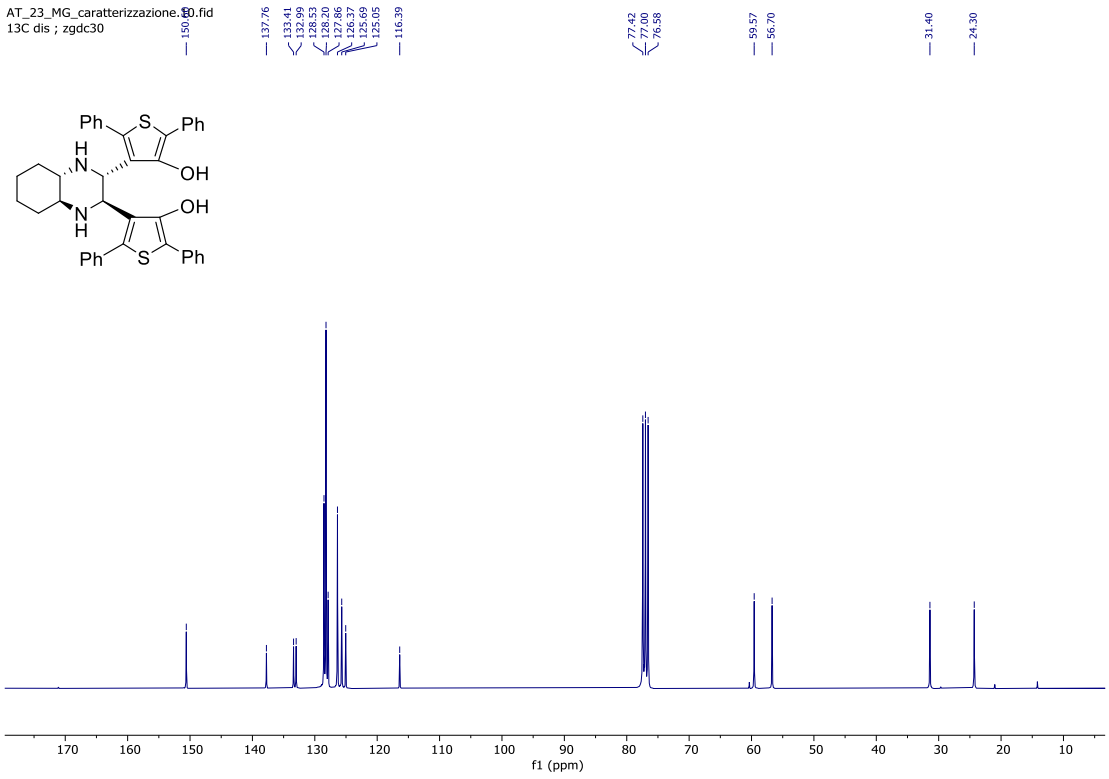

^{1}H-NMR compound 11

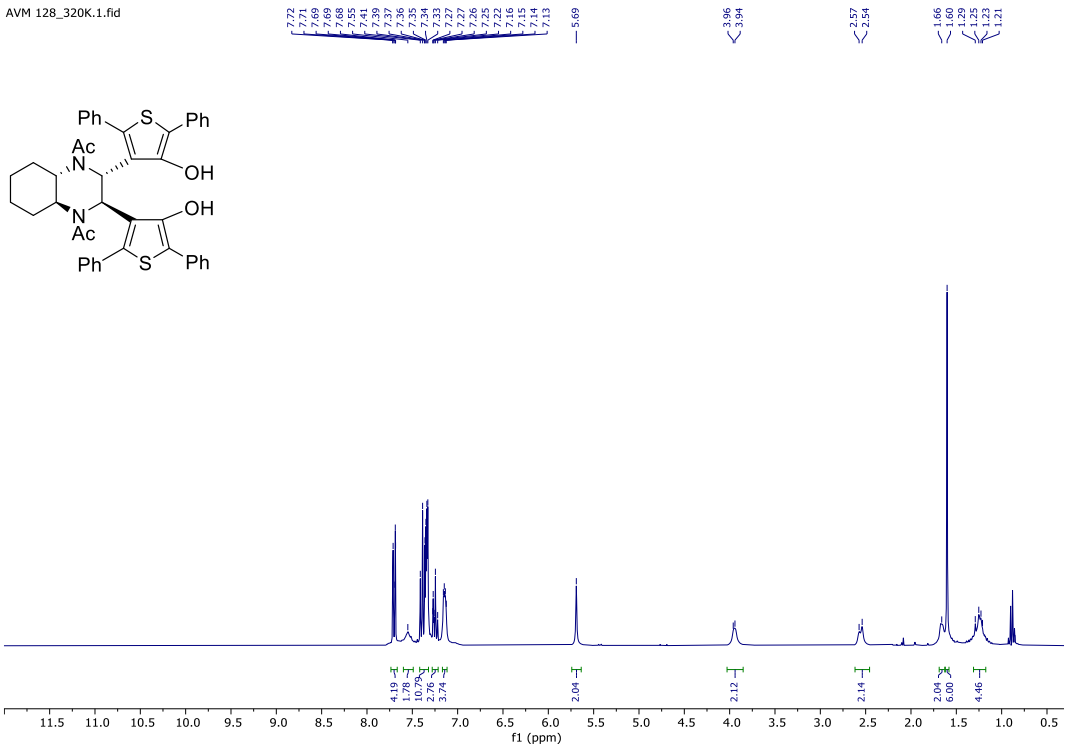

^{13}C-NMR compound 11

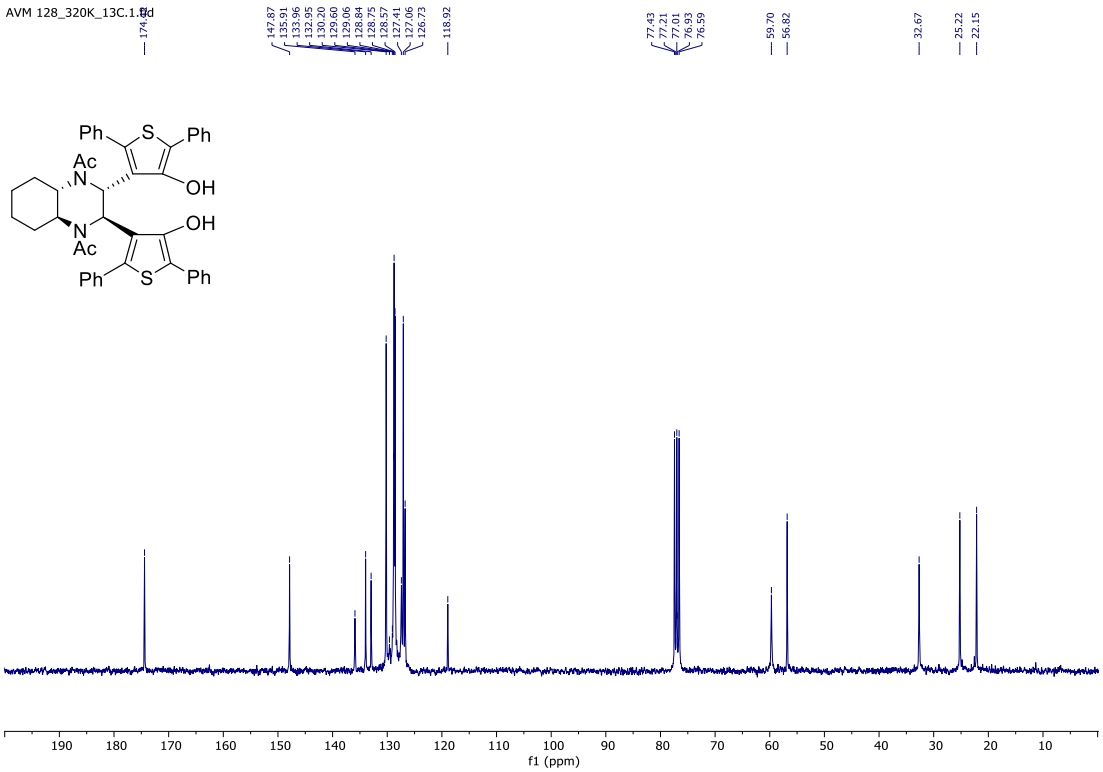

^{1}H-NMR compound 2

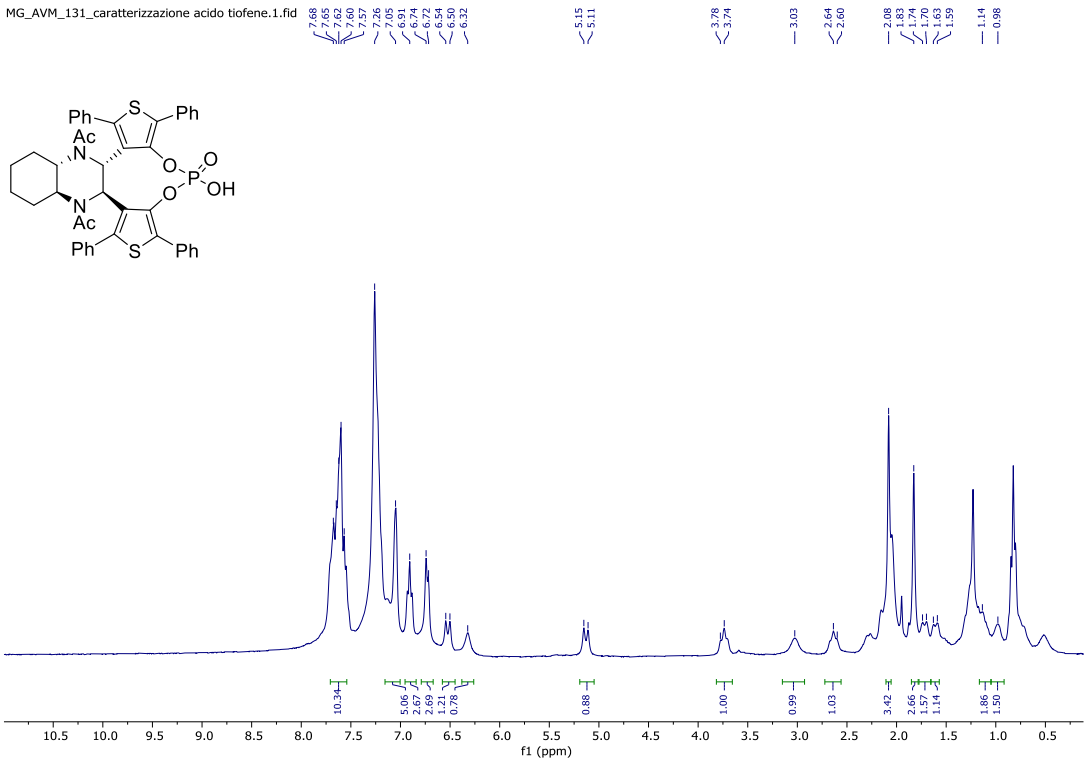

^{13}C-NMR compound 2

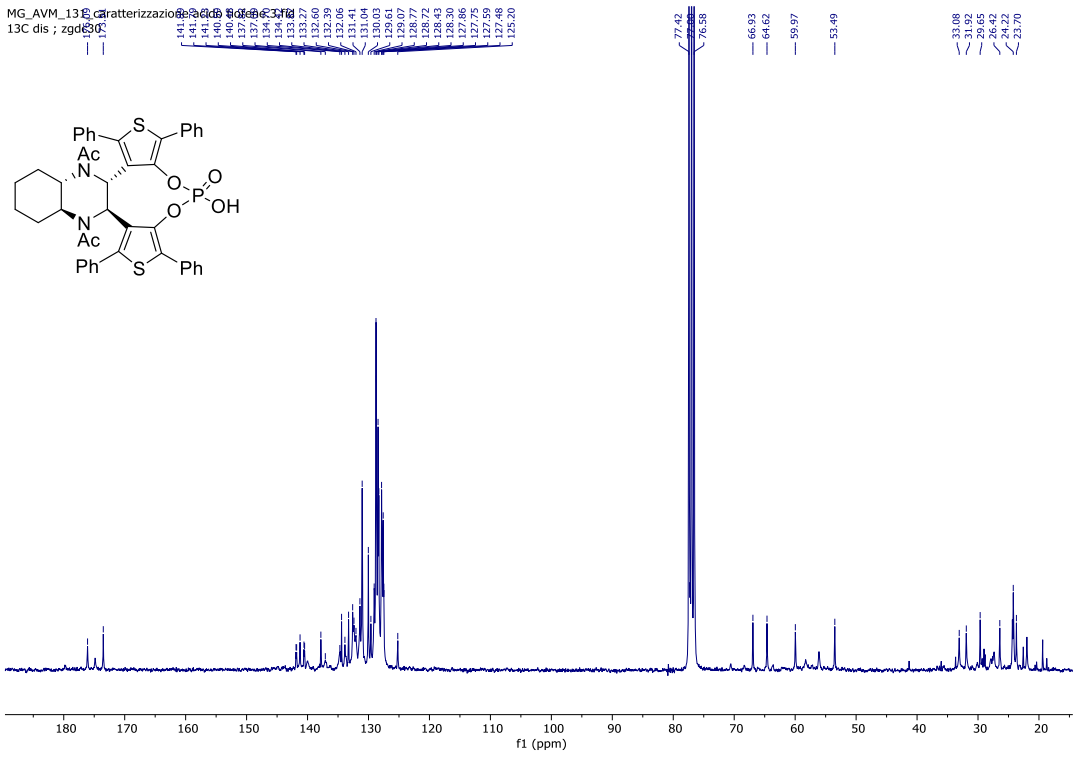

^{31}P-NMR compound 2

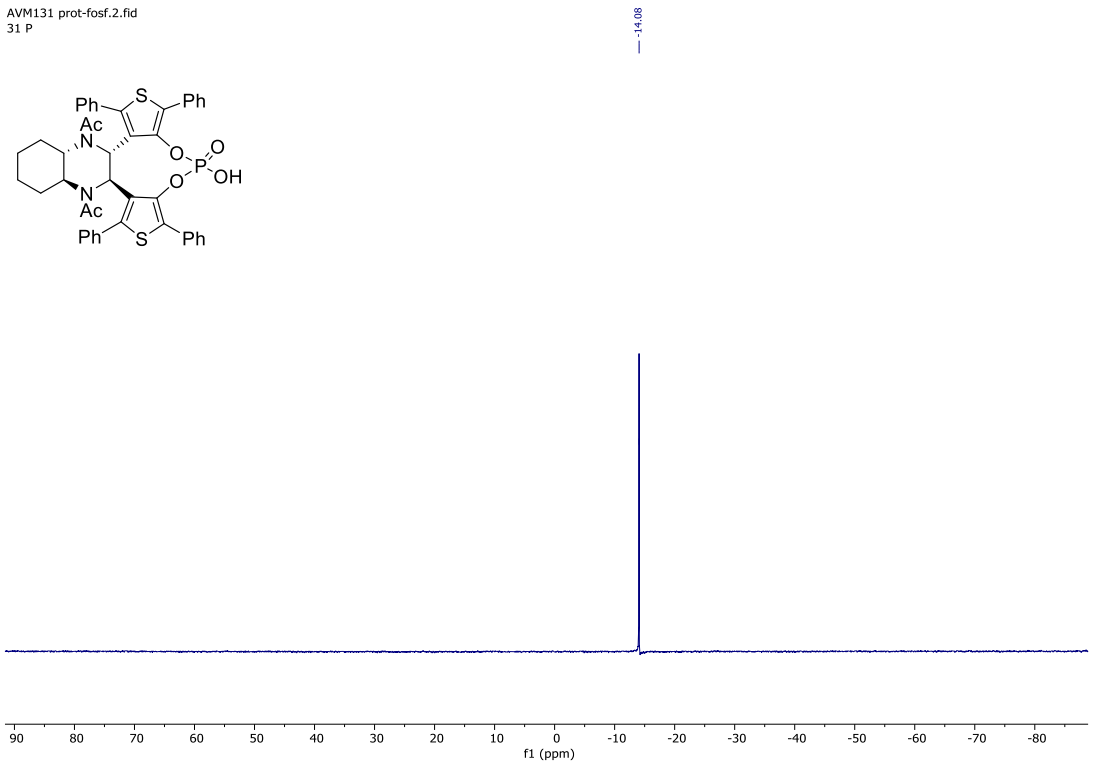

HRMS compound 6

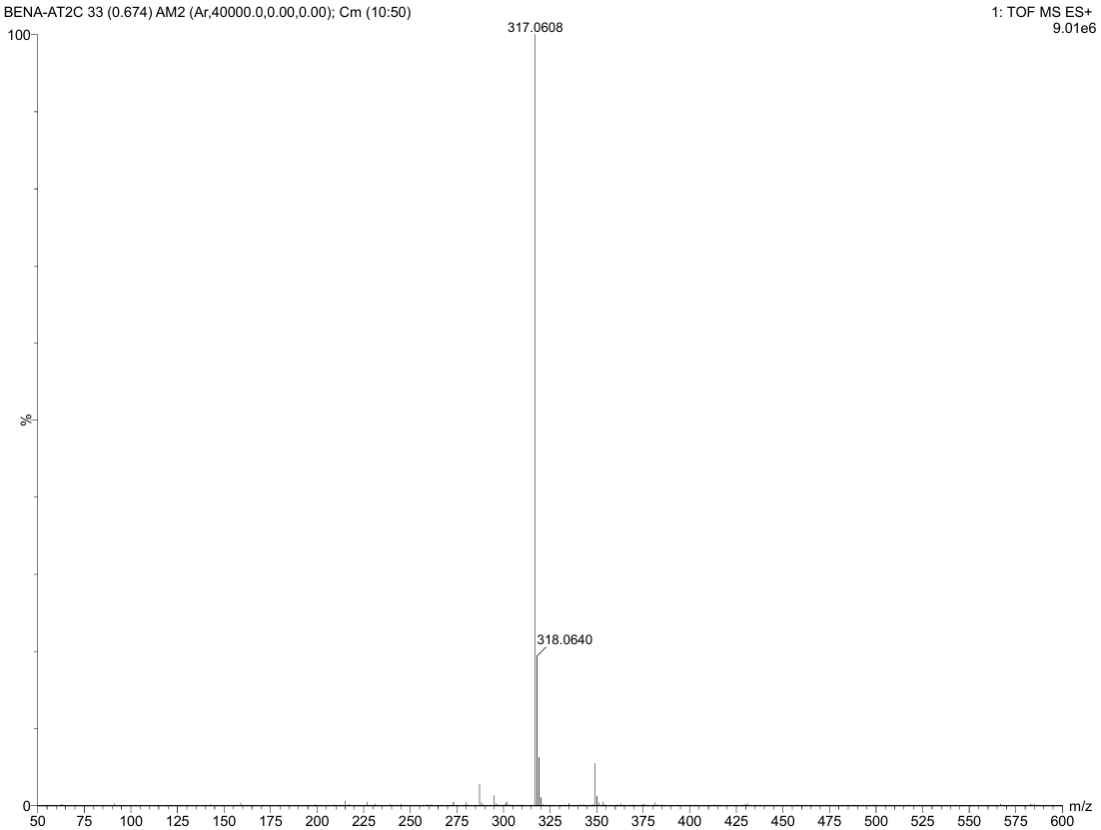

HRMS compound 7

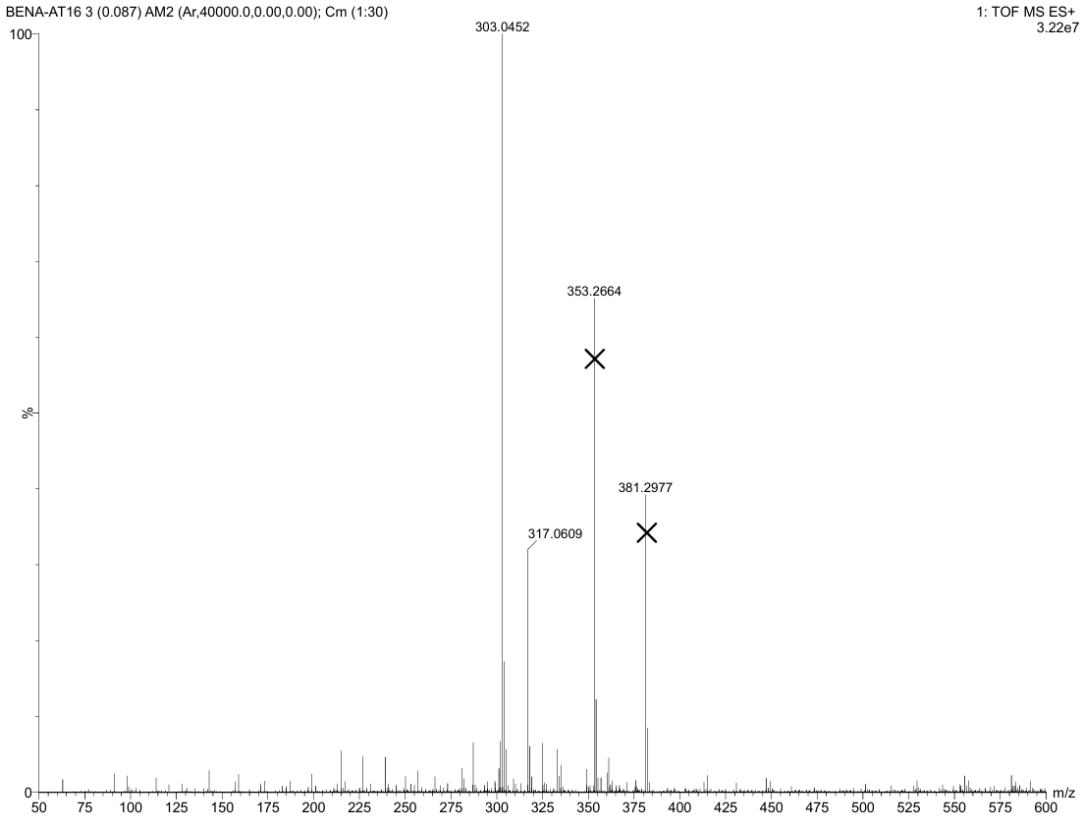

HRMS compound 9

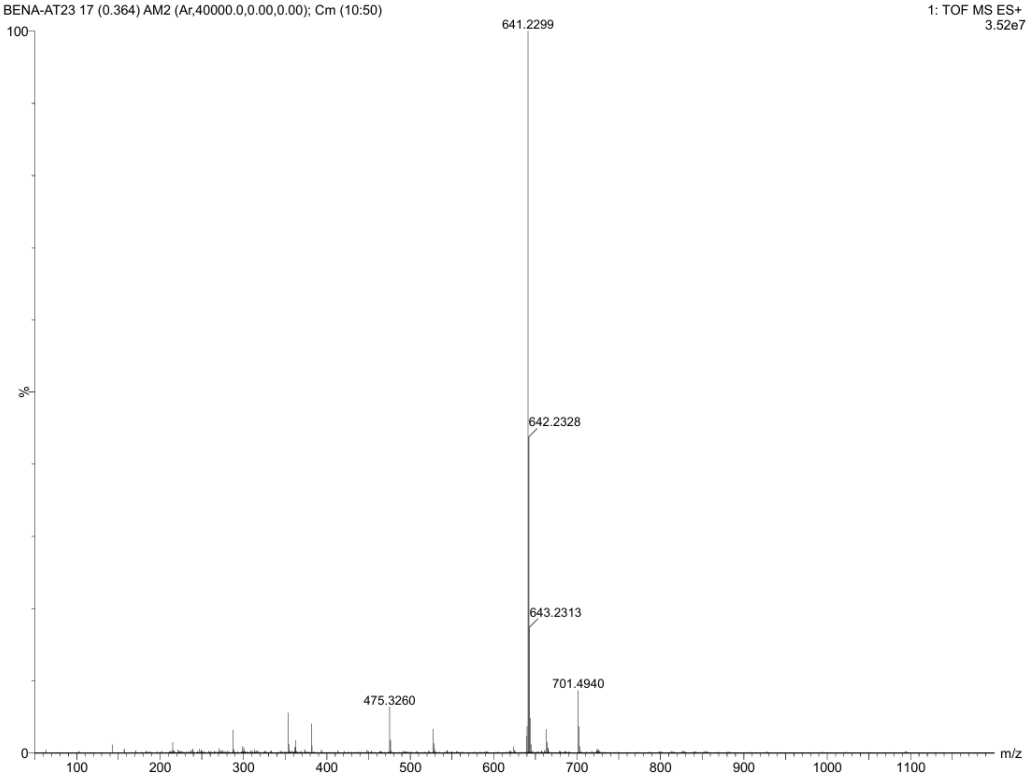

HRMS compound 11

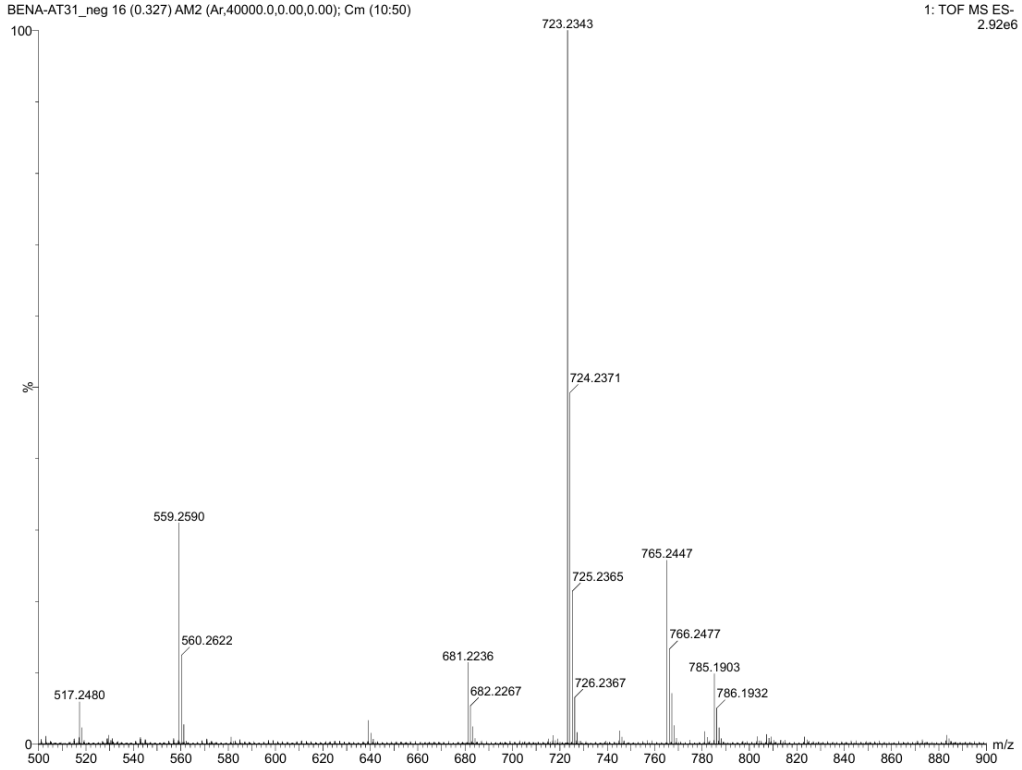

HRMS compound 2

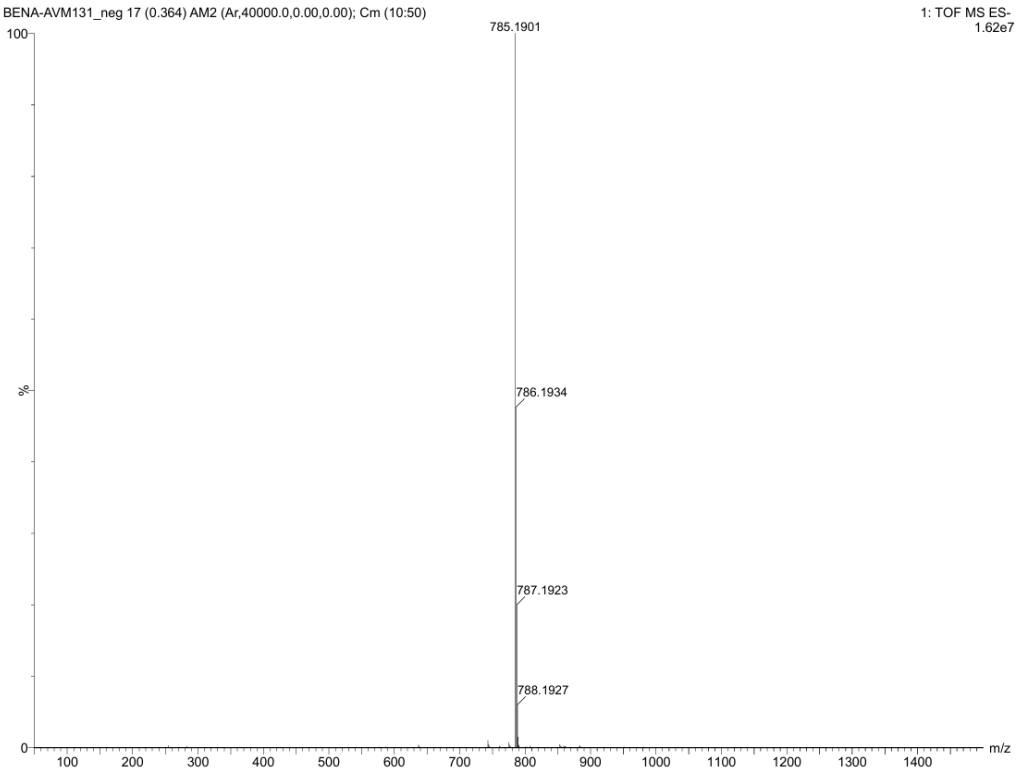

4. HPLC traces

HPLC compound 15aa

Daicel Chiralcel OD-H, Hexane/IPA 70:30, flow 0.6 mL/min, λ = 254 nm

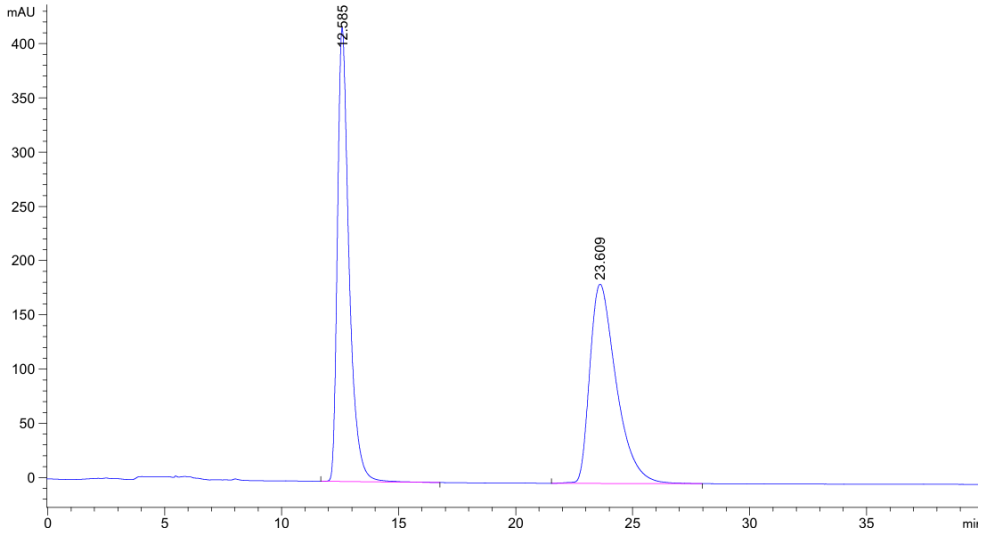

Peak #	RetTime [min]	Type	Width [min]	Area [mAU*s]	Height [mAU]	Area %
1	12.585	BB	0.5178	1.44145e4	418.50940	49.9997
2	23.609	BB	1.1773	1.44146e4	183.73701	50.0003

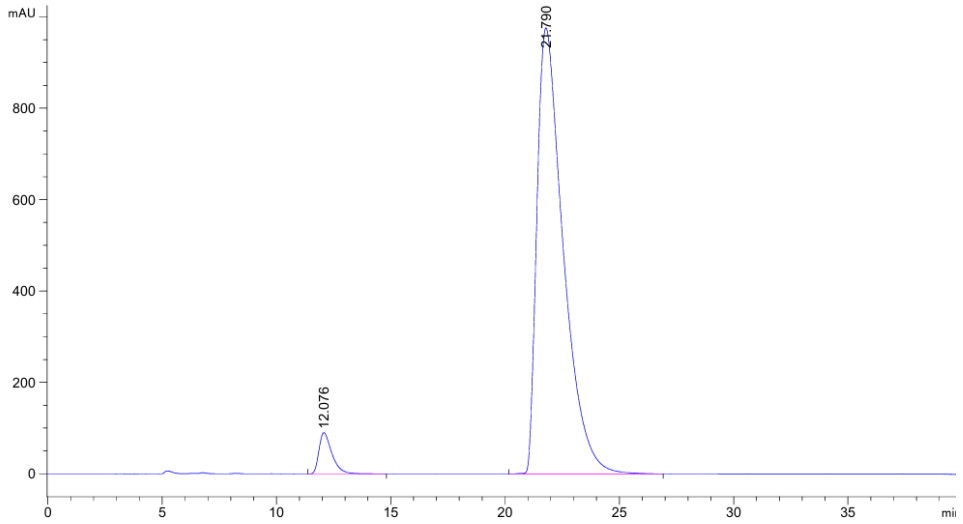

Peak #	RetTime [min]	Type	Width [min]	Area [mAU*s]	Height [mAU]	Area %
1	12.076	BB	0.5941	3570.79468	90.15186	4.3792
2	21.790	BB	1.1519	7.79684e4	976.15631	95.6208

HPLC compound 15ba

Phenomenex Lux Cellulose-1 3µm, Hexane/IPA 60:40, 0.75 mL/min, λ = 254 nm

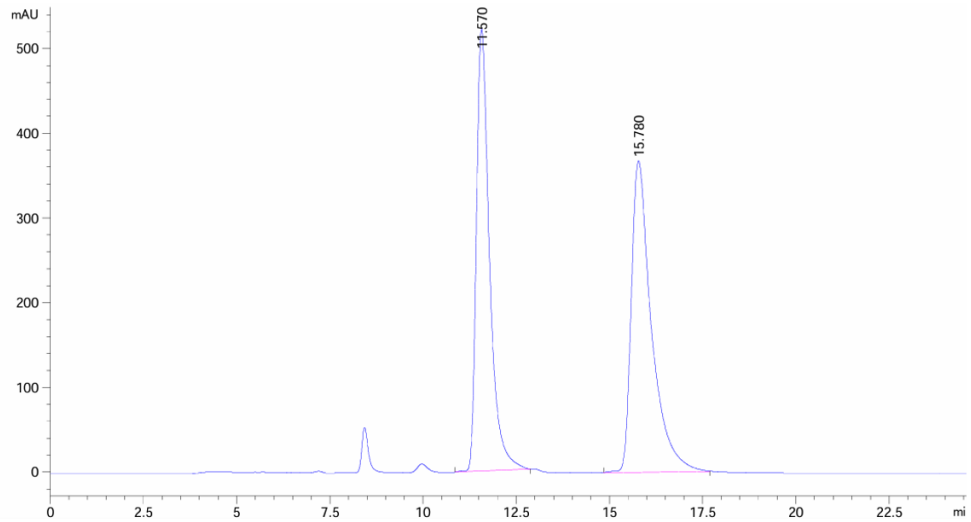

Peak #	RetTime [min]	Type	Width [min]	Area [mAU*s]	Height [mAU]	Area %
1	11.570	BB	0.3687	1.27316e4	521.76721	47.9717
2	15.780	BB	0.5520	1.38082e4	367.82962	52.0283

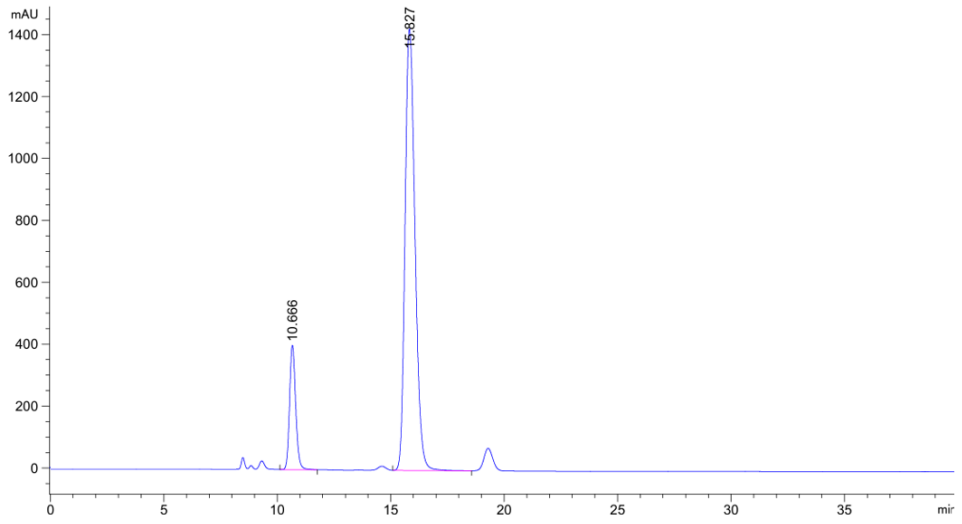

Peak #	RetTime [min]	Type	Width [min]	Area [mAU*s]	Height [mAU]	Area %
1	10.666	BB	0.2894	7556.23730	401.76801	14.7741
2	15.827	VB	0.4783	4.35889e4	1427.31543	85.2259

HPLC compound 15ca

Phenomenex Lux Cellulose-1 3µm, Hexane/IPA 70:30, 0.75 mL/min, λ = 254 nm

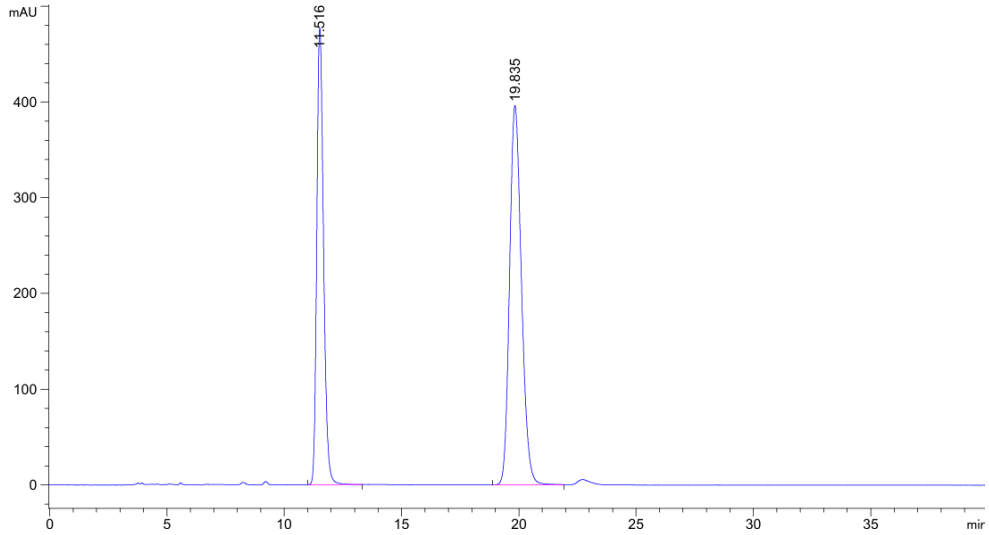

Peak #	RetTime [min]	Type	Width [min]	Area [mAU*s]	Height [mAU]	Area %
1	11.516	BB	0.3067	9522.52148	477.34512	49.9997
2	19.835	BB	0.5439	1.39204e4	396.20026	50.0003

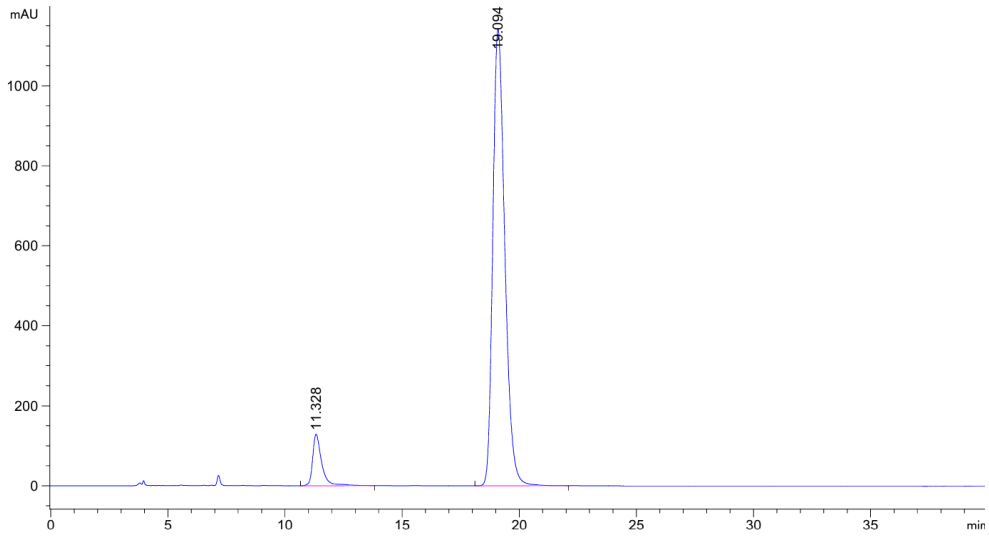

Peak #	RetTime [min]	Type	Width [min]	Area [mAU*s]	Height [mAU]	Area %
1	11.328	BB	0.3961	3469.67896	128.85759	7.8737
2	19.094	BB	0.5487	4.05971e4	1142.02686	92.1263

HPLC compound 15ab

Daicel Chiralcel OD-H, Hexane/IPA 80:20, flow 1.0 mL/min, λ = 254 nm

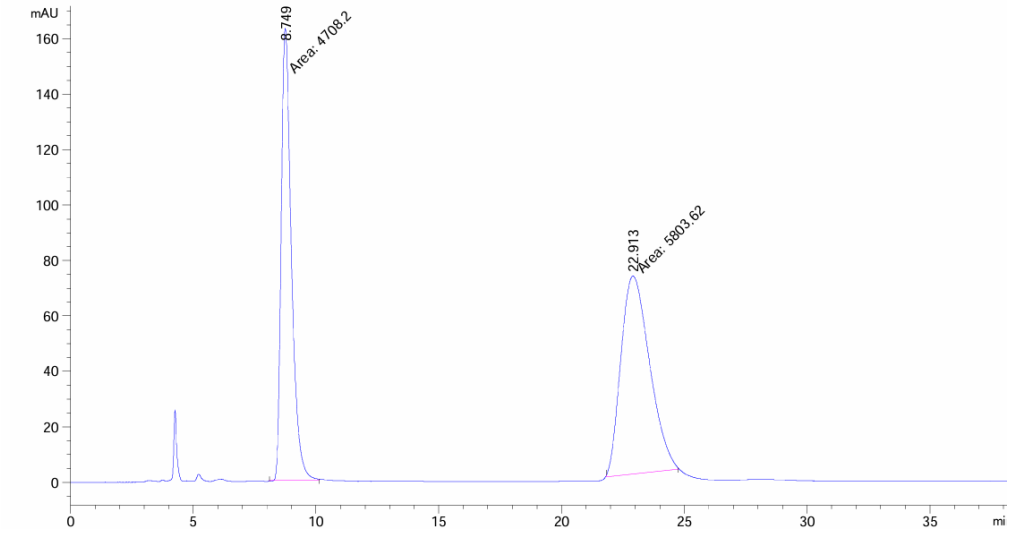

Peak #	RetTime [min]	Type	Width [min]	Area [mAU*s]	Height [mAU]	Area %
1	8.749	MM	0.4812	4708.20264	163.06223	44.7896
2	22.913	MM	1.3542	5803.62402	71.42915	55.2104

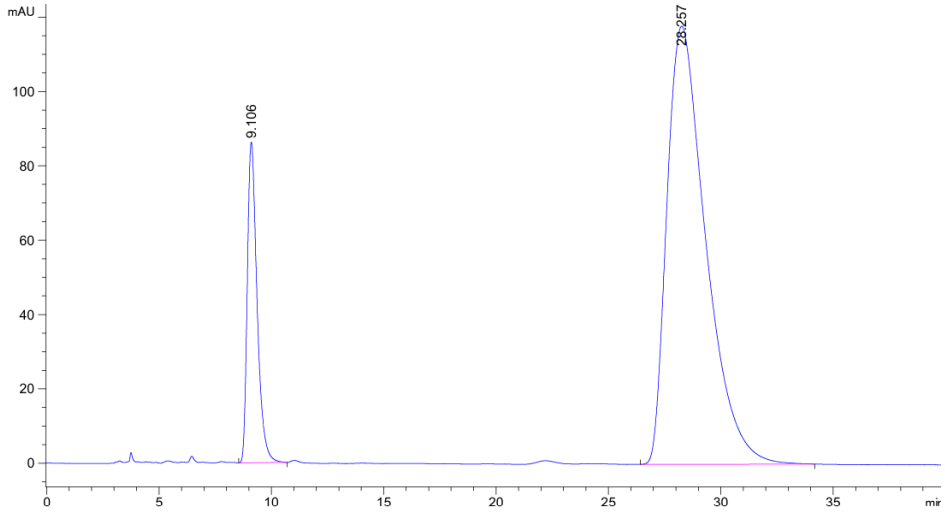

Peak #	RetTime [min]	Type	Width [min]	Area [mAU*s]	Height [mAU]	Area %
1	9.106	BB	0.4595	2598.51050	86.25161	15.5236
2	28.257	BB	1.7637	1.41406e4	117.86375	84.4764

HPLC compound 15ac

Daicel Chiralcel OD-H, Hexane/IPA 70:30, flow 0.8 mL/min, λ = 254 nm

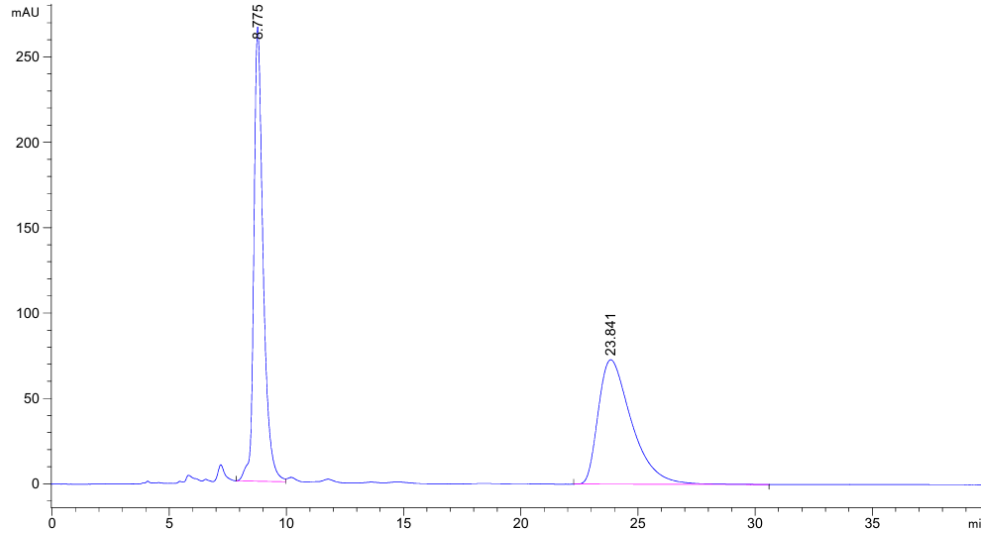

Peak #	RetTime [min]	Type	Width [min]	Area [mAU*s]	Height [mAU]	Area %
1	8.775	BV	0.4140	7341.60547	265.98685	50.4983
2	23.841	BB	1.5034	7196.73047	72.92261	49.5017

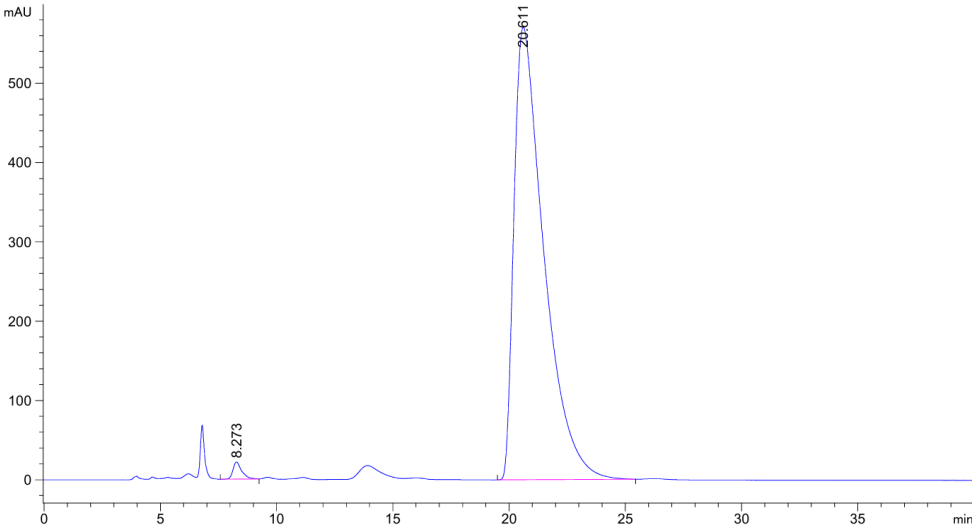

Peak #	RetTime [min]	Type	Width [min]	Area [mAU*s]	Height [mAU]	Area %
1	8.273	BB	0.3826	558.13837	21.51604	1.0807
2	20.611	BB	1.3078	5.10874e4	570.99963	98.9193

HPLC compound 15ad

Daicel Chiralcel OD-H, Hexane/IPA 60:40, flow 0.6 mL/min, λ = 280 nm

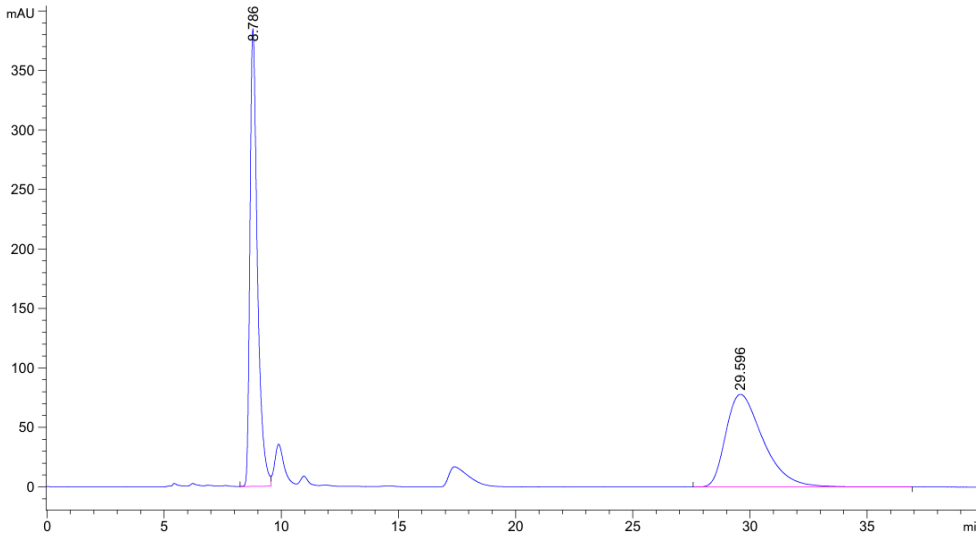

Peak #	RetTime [min]	Type	Width [min]	Area [mAU*s]	Height [mAU]	Area %
1	8.786	BV	0.3344	8517.40039	384.51608	49.6639
2	29.596	BB	1.7005	8632.70020	77.92422	50.3361

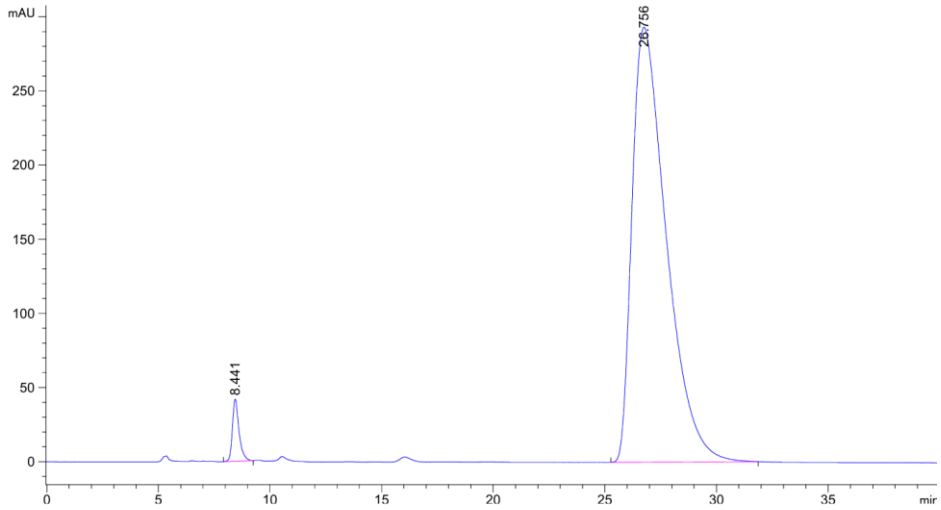

Peak #	RetTime [min]	Type	Width [min]	Area [mAU*s]	Height [mAU]	Area %
1	8.441	BB	0.3088	864.32684	41.87000	2.6911
2	26.756	BB	1.5154	3.12537e4	293.25534	97.3089

5. DFT Calculations

5.1. Buried volume analysis

Buried volume was calculated using SambVca 2.1 web application.[6] Conformational geometries of the decahydroquinoxaline-based chiral phosphoric acid **2** were obtained by Monte Carlo conformational analysis performed with Molecular Mechanics calculations using the OPLS2005 force field of the Macromodel package in the Schrodinger suite. These structures were then fully optimized by the DFT approach using the M06-2X functional in combination with the 6-31G+(d) basis set implemented in the Gaussian software package. Harmonic vibrational frequency calculations were also performed at the same level of theory to confirm that the obtained geometries correspond to a minimum (no imaginary frequencies). All calculations were conducted in vacuo. For the SambVca 2.1 analysis of decahydroquinoxaline-based CPAs, the following parameters were employed (**Figure S1**):

- Select the atoms coordinated to the center of the sphere: Phosphorous atom
- Select the atoms for z axis definition: The Z-axis is defined by the hydrogen of the stereogenic carbon on the decahydroquinoxaline scaffold, which lies in the same plane as the OH group and the phosphorus atom. This orientation was chosen to bisect the O=$\widehat{P}$-OH angle. (Z-negative)
- Select the atoms for xz-plane definition: XZ-plane defined by one oxygen atom of the phenol moiety
- Select the atoms to be deleted: none (default option)
- Select the atomic radii: Bondi radii scaled by 1.17 (default option)
- Sphere radius: 4.5 Å
- Distance of the coordination point from the center of the sphere: 2.0 Å. The selection of this distance was made to reflect the fact that substrates coordination does not occur directly at the phosphorus atom, but at the Lewis Acid site and at the Bronsted acid site of the catalyst.
- Mesh spacing for numerical integration: 0.05 Å
- No hydrogen atoms included in the calculation (default option)

%V_{Buried} calculated according to these parameters is reported in **Table S2**. In addition, the corresponding steric map is presented. The maps are oriented along the Z-axis, with red and blue regions denoting the more and less sterically hindered areas of the catalytic pocket, respectively. The label positioned in the corner of each map indicates the distance from the center of the sphere, expressed in Ångströms.

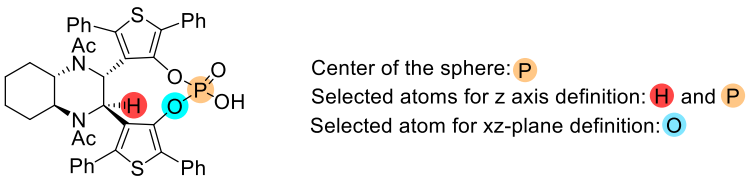

Figure S1. Graphical representation of atoms used for defining the Z-axis and XZ-plane, applied in the V_{buried} calculation for CPA **2**

Table S2. $\%V_{Buried}$ value calculated for decahydroquinoxaline-based CPA **2**

Compound	$\%V_{Free}$	$\%V_{Buried}$
Catalyst 2	59.9	40.1

Catalyst 2

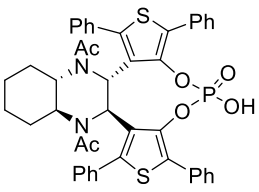

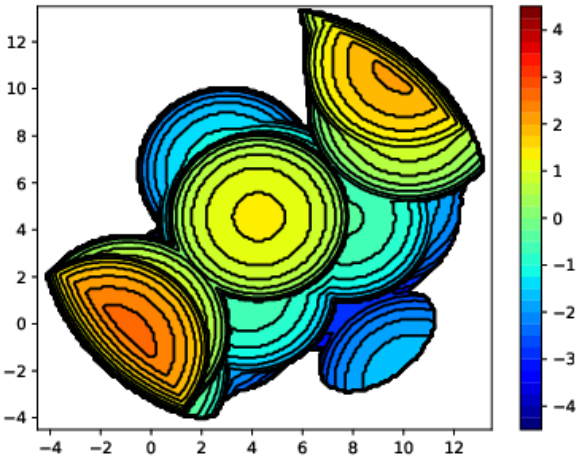

5.2. Transition State investigation

Conformational searches of the preliminary geometries of (catalyst **2**):(indole **14a**):(imine **13a**) complexes were performed employing a Monte Carlo sampling approach, using the OPLS2005 molecular mechanics force field as implemented in the Macromodel module of the Schrödinger suite. The lowest-energy thus obtained conformers (below 3.0 kcal/mol) were subjected to geometry optimization, and the Gibbs free energies of the corresponding transition states were initially estimated through the semiempirical PM6 method.

Initially, a constrained optimization was carried out, fixing the distance between the reaction carbons of indole **14a** and imine **13a** to 1.9 Å. After that, the constrain was removed and the structure was fully optimized in search of a first-order saddle point, which displayed an imaginary frequency corresponding to the vibration of the forming C-C bond between the reactants. Subsequently, full geometry optimizations were carried out by DFT approach, using M06-2X functional in combination with the 6-31G(d) basis set. Harmonic vibrational frequency calculations were carried out at the same level of theory to verify the nature of the transition states, which was confirmed by the presence of a single imaginary frequency. From these optimized structures, single-point energy calculations were subsequently performed at M06-2X/6-311++G(2d,2p) level of theory in order to refine the electronic energy values. The final Gibbs free energy for each of the 8 transition state structures was computed by summing the single-point electronic energy obtained at M06-2X/6-311++G(2d,2p) level with the thermal correction to Gibbs free energy derived from the vibrational analysis at the M06-2X/6-31G(d) level. All calculations were performed in the gas phase under standard conditions.

In order to ensure to identify all transition-state geometries, for each coordination model proposed related to the enantioselective addition of indoles to *N*-tosylimines, an exhaustive conformational search was undertaken. Both *Z* and *E* isomers of the imine were considered (even if imine **13a** adopts the *E* configuration), along with two distinct relative orientations of the indole. Specifically, when the C=N-Tos group of the imine overlaps with the five-membered ring of the indole, the arrangement is described as *endo*; otherwise, when no such overlap occurs, the orientation is referred to as *exo*.[7] In addition, for each conformer, two possible diastereomeric transition states are possible according to the (*R*) or (*S*) enantiomer of product **15aa** formed (**Figure S2**).

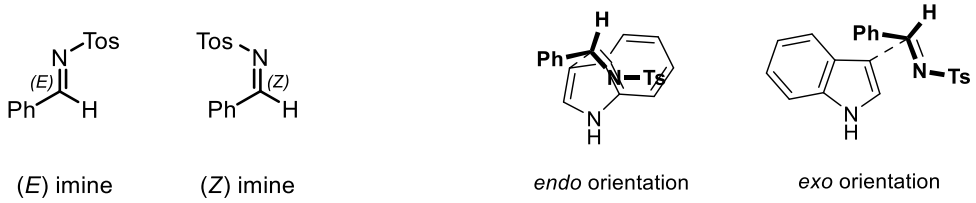

Figure S2. Competing conformations for the transition state of the reaction

The studied coordination model reflects the classical coordination model proposed by Simon and Goodman,[7] in which the imine is activated via hydrogen bonding at the Brønsted acid site of the catalyst. A schematic overview of the transition state geometries proposed according to this coordination model is presented in **Scheme S1**, while the corresponding energy values are summarized in **Table S3**.

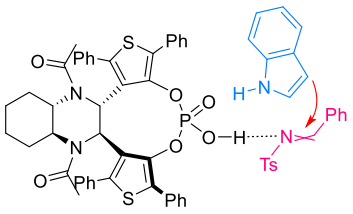

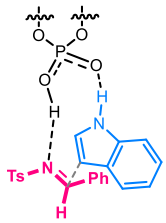

TS1-*E*-*exo*-(*S*)

ΔΔG 4.28 kcal/mol

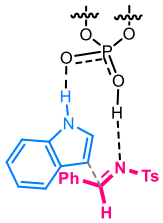

TS2-*E*-*exo*-(*R*)

ΔΔG 4.25 kcal/mol

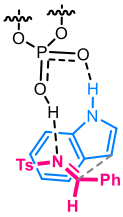

TS3-*E*-*endo*-(*S*)

ΔΔG 0.00 kcal/mol

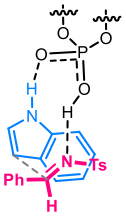

TS4-*E*-*endo*-(*R*)

ΔΔG 1.35 kcal/mol

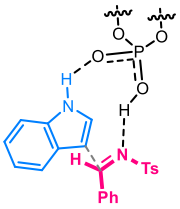

TS5-*Z*-*exo*-(*S*)

ΔΔG 11.18 kcal/mol

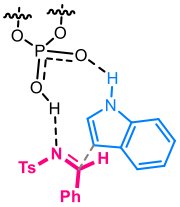

TS6-*Z*-*exo*-(*R*)

ΔΔG 11.17 kcal/mol

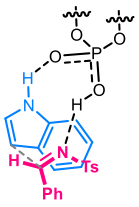

TS7-*Z*-*endo*-(*S*)

ΔΔG 14.87 kcal/mol

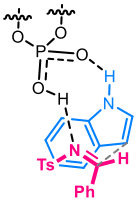

TS8-*Z*-*endo*-(*R*)

ΔΔG 8.79 kcal/mol

Scheme S1. Computed transition states for the Friedel-Craft addition of *N*-tosylimine **13a** to indole **14a**. The *E* and *Z* in the names refer to the configuration of the imine double bond, whereas the (*R*) and (*S*) description refers to the final configuration of product **15aa**. In the competing conformations for the transition states, decahydroquinoxaline scaffold omitted for clarity; ΔΔG values (in vacuo) are expressed in kcal mol^{-1} and calculated at M06-2X/6-311G(++)(2d,2p)//M06-2X/6-31G(d) level of theory. See **Table S3** for further details.

In **Table S3**, for each of the 8 calculated transition state structures, the thermal correction to the Gibbs free energy, the energy value, the Gibbs free energy, ΔΔG values and the vibrational analysis are reported. ΔΔG can be defined as the Gibbs free energy difference between a generic transition state and the transition state with the lowest Gibbs free energy.

Table S3. Complete overview of the thermal corrections to the Gibbs free energy, the energy values, the Gibbs free energies, ΔΔG values and the vibrational analyses of the 8 transition state structures

	M06-2X / 6-31G(d) 25°C	M06-2X / 6-311G(++)(2d,2p) 25°C			
TS #	Thermal correction (kcal/mol)	ΔE (kcal/mol)	ΔG (kcal/mol)	ΔΔG (kcal/mol)	Frequency (cm^{-1})
TS1-*E-exo-(S)*	646,9949	-3.079.224,5714	-3078577,5765	4,28	-254.79
TS2-*E-exo-(R)*	647,0357	-3.079.224,6486	-3078577,6129	4,25	-212.45
TS3-*E-endo-(S)*	643,0466	-3.079.224,9065	-3078581,8599	0,00	-134.55
TS4-*E-endo-(R)*	644,1856	-3.079.224,6957	-3078580,5101	1,35	-105.96
TS5-*Z-exo-(S)*	645,5328	-3.079.216,2174	-3078570,6846	11,18	-184.57
TS6-*Z-exo-(R)*	645,8491	-3.079.216,5387	-3078570,6896	11,17	-209.14
TS7-*Z-endo-(S)*	648,2493	-3.079.215,2416	-3078566,9923	14,87	-283.54
TS8-*Z-endo-(R)*	644,2540	-3.079.217,3205	-3078573,0666	8,79	-136.76

5.3. Enantiomeric excess calculation

The enantiomeric excess was calculated at M06-2X / 6-311G(++)(2d,2p) level of theory using the relative Gibbs free energies of **TS1-TS8** previously calculated under vacuo. For each transition state, the relative rate constant (k) was determined using the Eyring equation:

$$k \propto e^{-\frac{\Delta G^{\ddagger}}{RT}}$$

Where:

$\Delta G^{\ddagger}$ is the Gibbs free energy of a transition state in kcal/mol

R is the gas constant = 0.001987204 kcal/mol·K

T is the temperature in Kelvin (-50 °C = 223.15 K)

The overall rate for the formation of the (*R*)-enantiomer was calculated as a sum of the rate constants associated with all transition states leading to the (*R*)-product (**Table S4**). Similarly, the overall rate for the formation of the (*S*)-enantiomer was obtained as a sum of the rate constants corresponding to the transition states leading to the (*S*)-product (**Table S5**).

$$k_{tot}(R) = k_1(R) + k_2(R) + \ \ldots$$

$$k_{tot}(S) = k_1(S) + k_2(S) + \ \ldots$$

The *ee* was then calculated as:

$$ee(S) = \frac{k_{tot}(S) - k_{tot}(R)}{k_{tot}(S) + k_{tot}(R)} * 100$$

Table S4. Overall rate for the formation of the (*R*)-enantiomer calculated at M06-2X / 6-311G(++)(2d,2p) level of theory

TS #	$\Delta G^{\ddagger}$ (kcal/mol)	$\Delta\Delta G^{\ddagger}$ (kcal/mol)	e-$\Delta G^{\ddagger}$/RT (kcal/mol)
TS2-*E-exo-(R)*	-3078577,6129	4,25	6,92865E-05
TS4-*E-endo-(R)*	-3078580,5101	1,35	0,047651713
TS6-*Z-exo-(R)*	-3078570,6896	11,17	1,14866E-11
TS8-*Z-endo-(R)*	-3078573,0666	8,79	2,44428E-09
		$k_{tot}(R)$	0,047721

Table S5. Overall rate for the formation of the (*S*)-enantiomer calculated at M06-2X / 6-311G(++)(2d,2p) level of theory

TS #	$\Delta G^{\ddagger}$ (kcal/mol)	$\Delta\Delta G^{\ddagger}$ (kcal/mol)	e-$\Delta G^{\ddagger}$/RT (kcal/mol)
TS1-*E-exo-(S)*	-3078577,5765	4,28	6,3827E-05
TS3-*E-endo-(S)*	-3078581,8599	0,00	1
TS5-*Z-exo-(S)*	-3078570,6846	11,18	1,13573E-11
TS7-*Z-endo-(S)*	-3078566,9923	14,87	2,74915E-15
		$k_{tot}(S)$	1,000064

According to these calculations the enantiomeric excess calculated for the Friedel-Crafts addition of *N*-tosilimine **13a** to indole **14a** promoted by catalyst **2**, was found to be 91 % for (*S*)-**15aa** product.

To obtain a more accurate estimate of the enantiomeric excess, all the transition states **TS1-TS8** were calculated at the M06-2X / 6-311G(++)(2d,2p) level of theory in dichloromethane as solvent, which was incorporated using the PCM model. The resulting Gibbs free energies of the transition states are reported in **Table S6** and **Table S7**. The calculated enantiomeric excess was found to be 91 % for (*S*)-**15aa** product also in this case.

Table S6. Overall rate for the formation of the (*R*)-enantiomer calculated at M06-2X/6-311G(++)(2d,2p) PCM (dichloromethane) level of theory

TS #	$\Delta G^{\ddagger}$ (kcal/mol)	$\Delta\Delta G^{\ddagger}$ (kcal/mol)	e-$\Delta G^{\ddagger}$/RT (kcal/mol)
TS2-*E-exo-(R)*	-3078592,6731	6,97	1,49726E-07
TS4-*E-endo-(R)*	-3078598,2761	1,37	0,045995409
TS6-*Z-exo-(R)*	-3078584,8246	14,82	3,07431E-15
TS8-*Z-endo-(R)*	-3078591,8747	7,77	2,468E-08
		$k_{tot}(R)$	0,045996

Table S7. Overall rate for the formation of the (*S*)-enantiomer calculated at M06-2X/6-311G(++)(2d,2p) PCM (dichloromethane) level of theory

TS #	$\Delta G^{\ddagger}$ (kcal/mol)	$\Delta\Delta G^{\ddagger}$ (kcal/mol)	e-$\Delta G^{\ddagger}$/RT (kcal/mol)
TS1-*E-exo-(S)*	-3078593,3351	6,31	6,66282E-07
TS3-*E-endo-(S)*	-3078599,6416	0,00	1
TS5-*Z-exo-(S)*	-3078585,4348	14,21	1,21992E-14
TS7-*Z-endo-(S)*	-3078585,2253	14,42	7,60552E-15
		$k_{tot}(S)$	1,000001

5.4. Computational pKa determination

The initial conformational geometries were obtained through Monte Carlo conformational analysis performed with Molecular Mechanics calculations using the OPLS2005 force field[8] of the Macromodel package[9] in the Schrodinger suite.[10] For molecules exhibiting multiple conformers, the structure within 3 kcal/mol were fully optimized by DFT calculations in gas-phase using the M06-2X functional[11] with the 6-31+G(d) basis set implemented in the Gaussian package.[12]

5.4.1. pKa values computed according to the isodesmic method

Harmonic vibrational frequency calculations were performed at the same level of theory to confirm the nature of the stationary points and to obtain thermal corrections to the Gibbs free energy and the structure with the lowest free Gibbs energy was selected for subsequent calculations.

Single-point energy calculations were subsequently carried out on the optimized structures at the M06-2X/6-311++G(2df,2p) level of theory, including solvent effects via the SMD solvation model[13] for DMSO and CH_3CN. The previously calculated thermal corrections were then added to the electronic energies to obtain the final Gibbs free energies used for pKa determination.

The conjugate base of **2** was generated by removing a proton from the corresponding acid structure. No conformational analysis was performed for it; geometry was directly reoptimized using the same DFT methodology described above.

This computational protocol was applied to investigate the acidic properties of decahydroquinoxaline-based chiral phosphoric acid **2**. The pKa values were computed in both DMSO and CH_3CN as solvent and results are reported in **Table S8**.

The energies calculated for the neutral chiral phosphoric acid **2** and the corresponding anion are reported in **Table S9** and **Table S10**.

Table S8. Computed pKa values of chiral phosphoric acid **2** in DMSO and CH3CN calculated at SMD / M06-2X/6-311++G(2df,2p) // M06-2X/6-31G+(d) level of theory according to the isodesmic approach

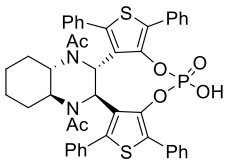

$pKa_{(calc)}$ DMSO	$pKa_{(calc)}$ CH_3CN
1,05	10,91

Table S9. Complete overview of the energies calculated for the neutral chiral phosphoric acid **2**

GAS PHASE (M062x 631g+ (d))		GAS PHASE (M062X6-311++G (2df,2p))		SMD (DMSO) (M062X6-311++G (2df,2p))		SMD (CH_3CN) (M062X6-311++G (2df,2p))	
Thermal correction to Free Energy (hartree)	ΔG (hartree)	ΔE (hartree)	ΔG (hartree)	ΔE (hartree)	ΔG (hartree)	ΔE (hartree)	ΔG (hartree)
0,6721	-3397,2591	-3.398,7494	-3.398,0773	-3398,7935	-3398,1214	-3398,8038	-3398,1317

Table S10. Complete overview of the energies calculated for the anion of chiral phosphoric acid **2**

GAS PHASE (M062x 631g+ (d))		GAS PHASE (M062X6-311++G (2df,2p))		SMD (DMSO) (M062X6-311++G (2df,2p))		SMD (CH_3CN) (M062X6-311++G (2df,2p))	
Thermal correction to Free Energy (hartree)	ΔG (hartree)	ΔE (hartree)	ΔG (hartree)	ΔE (hartree)	ΔG (hartree)	ΔE (hartree)	ΔG (hartree)
0,6615	-3396,7864	-3398,2579	-3397,5964	-3398,3493	-3397,6878	-3398,3574	-3397,6959

5.4.2. pKa values computed using the LFESR method

The Gibbs free energies of the protonated (HA) and deprotonated (A^-) species corresponding to chiral decahydroquinoxaline-based phosphoric acid **2** were recalculated through full geometry optimization and vibrational frequency analysis at the SMD/M06-2X/6-311++G(2df,2p) level of theory.

The resulting pKa values, corrected using the linear free energy scaling relationships, were computed in both DMSO and CH_3CN as solvent ($\Delta G(H^+)_{(DMSO)}$ = -11.1155416306813 eV, ($\Delta G(H^+)_{(CH3CN)}$ = -11.0855416306813 eV) and results are reported in **Table S11**.

These values require a linear free energy scaling correction to reduce systematic deviations arising from the intrinsic limitations of the implicit solvation model employed in the calculations. For DMSO and CH_3CN, the corrected pKa values are derived using a linear regression where:

$$pKa(DMSO) = 0.7517\ pKa_{calc}(DMSO) - 6.1$$

$$pKa(CH_3CN) = 0.8115\ pKa_{calc}(CH_3CN) + 2.3$$

All the energies calculated for the neutral chiral phosphoric acid **2** and the corresponding anion are reported in **Table S12**.

Table S11. Computed pKa values in DMSO for chiral phosphoric acid **2** performed at SMD / M06-2X/6-311++G(d,p) level of theory according to LFESR approach

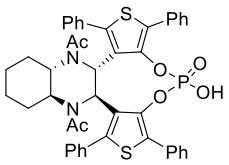

pKa $_{(LFESR)}$ DMSO	pKa $_{(LFESR)}$ CH_3CN
1,36	10,99

Table S12. Complete overview of the energies calculated for chiral phosphoric acid **2** and the corresponding anion

Free Gibbs energies in DMSO		Free Gibbs energies in CH_3CN	
ΔG_{HA} (hartree)	ΔG_{A^-} (hartree)	ΔG_{HA} (hartree)	ΔG_{A^-} (hartree)
-3397,9432	-3397,5131	-3397,9523	-3397,5218

6. Circular dichroism spectra

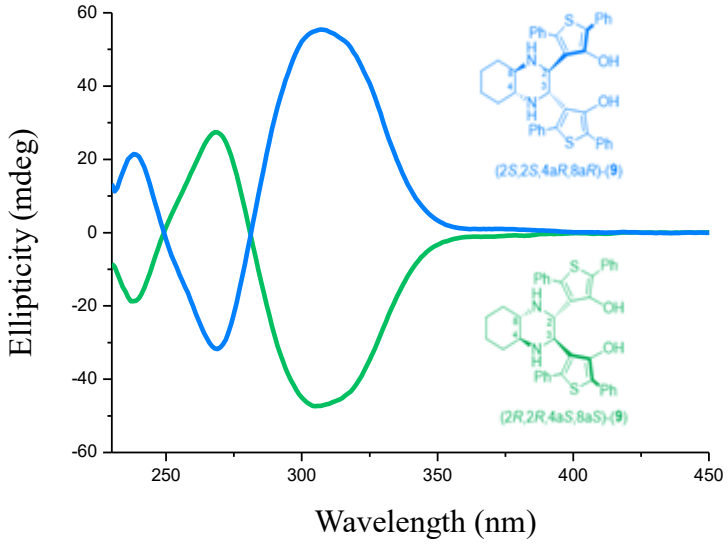

Figure S3. Circular dichroism spectra. Chromatographic conditions: column, Chiralpak IB column (250 mm x 4.6 mm); mobile phase, *n*-hexane/EtOH/DEA (100:10:0.1); temperature, 40 °C; flow rate, 1.0 mL/min; detection, CD at 280 nm

7. References

1. Gabrieli S.; Cirilli R.; Benincori T.; Pierini M.; Rizzo S.; Rossi S. *Eur. J. Org. Chem*. 2017, *2017*, 861 – 870.
2. Yanagisawa S.; Sudo T.; Noyori R.; Itami K. *J. Am. Chem. Soc*. 2006, *128*, 11748 – 11749.
3. Morales, S.; Guijarro, F. G.; García Ruano, J. L.; Cid, M. B. *J. Am. Chem. Soc.* 2014, *136*, 1082–1089.
4. Huang, D.; Wang, X.; Wang, X.; Chen, W.; Wang, X.; Hu, Y. *Org. Lett.* 2016, *18*, 604–607.
5. Kang, Q.; Zhao, Z.; You, S. *J. Am. Chem. Soc.* 2007, *129*, 1484–1485.
6. SambVca 2.1, https://www.aocdweb.com/OMtools/sambvca2.1/index.html
7. Simon, L.; Goodman, J. M. *J. Org. Chem.* 2010, *75*, 589–597.
8. M. Busch, E. Ahlberg, E. Ahlberg, K. Laasonen, *ACS Omega* 2022, *7*, 17369–17383.
9. J. L. Banks, H. S. Beard, Y. Cao, A. E. Cho, W. Damm, R. Farid, A. K. Felts, T. A. Halgren, D. T. Mainz, J. R. Maple, R. Murphy, D. M. Philipp, M. P. Repasky, L. Y. Zhang, B. J. Berne, R. A. Friesner, E. Gallicchio, R. M. Levy, *J Comput Chem* 2005, *26*, 1752–1780.
10. M. Busch, E. Ahlberg, K. Laasonen, *Phys Chem Chem Phys* 2021, *23*, 11727–11737.
11. Y. Zhao, D. G. Truhlar, *Theoretical Chemistry Accounts* 2007, *120*, 215–241.
12. Gaussian 16,Revision C.01, M. J. Frisch, G. W. Trucks, H. B. Schlegel, G. E. Scuseria, M. A. Robb, J. R. Cheeseman, G. Scalmani, V. Barone, G. A. Petersson, H. Nakatsuji, X. Li, M. Caricato, A. V. Marenich, J. Bloino, B. G. Janesko, R. Gomperts, B. Mennucci, H. P. Hratchian, J. V. Ortiz, A. F. Izmaylov, J. L. Sonnenberg, D. Williams-Young, F. Ding, F. Lipparini, F. Egidi, J. Goings, B. Peng, A. Petrone et al., Gaussian, Inc., Wallingford CT 2019.
13. Schrödinger Release 2024-1: MacroModel, Schrödinger, LLC, New York, NY, 2024.